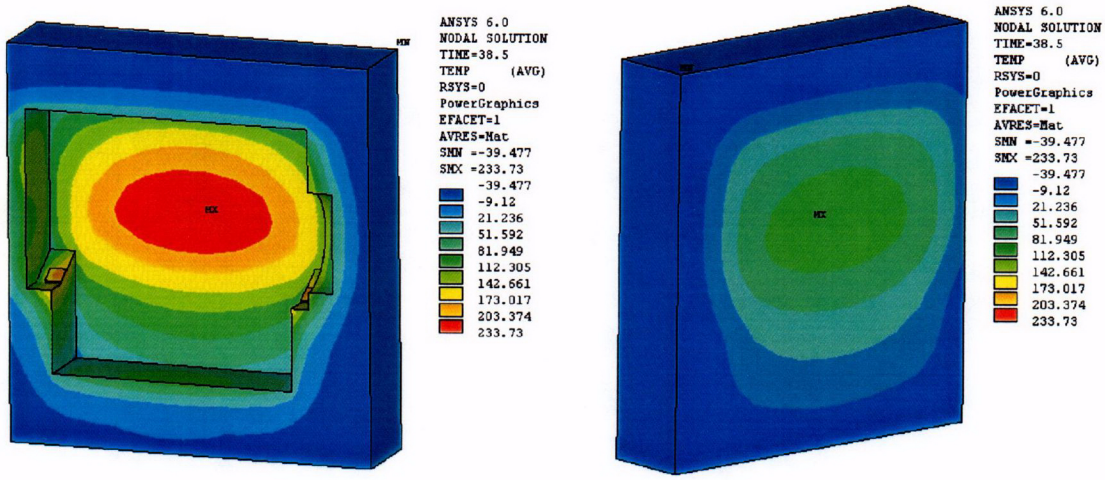

Figure P.4-17 Temperature Distribution in a Single HSM-H, 40.8 kW Heat Load, -40°F Ambient, Maximum Temperature Gradients through Concrete Walls. Blocked Vent Transient at 38.5 Hours

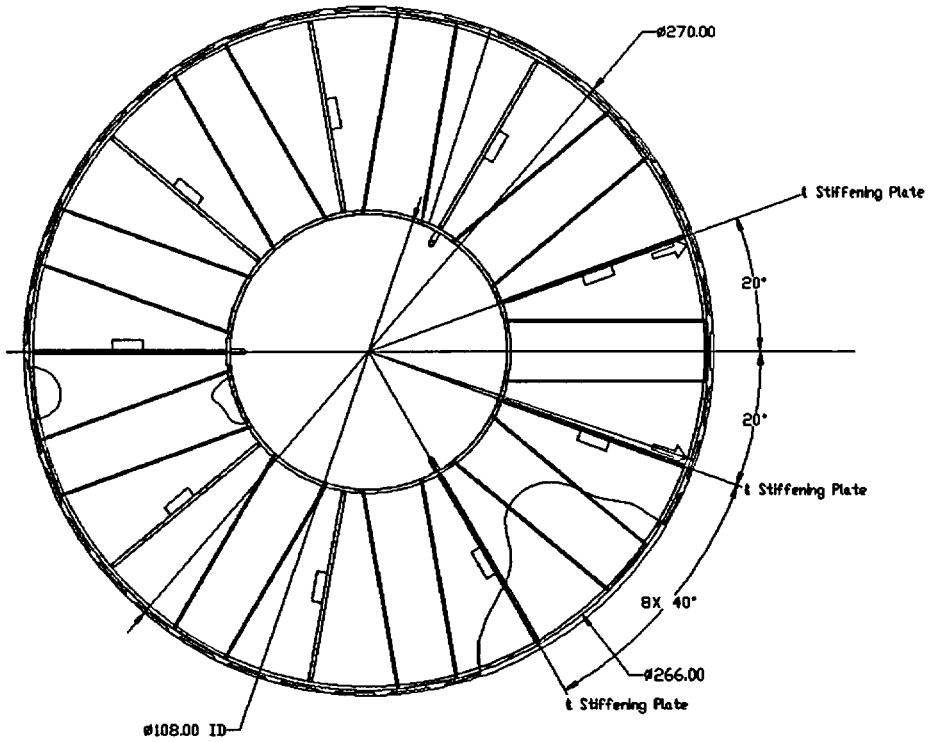

Plan View Of Short & Long Spacers

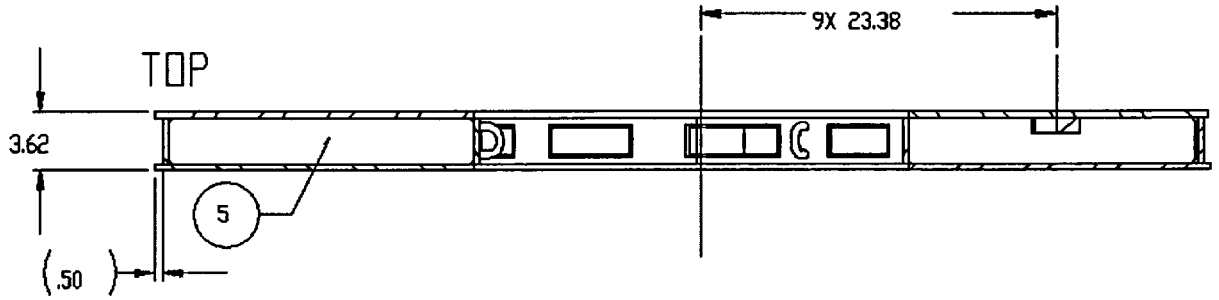

Elevation View Of Short Spacer

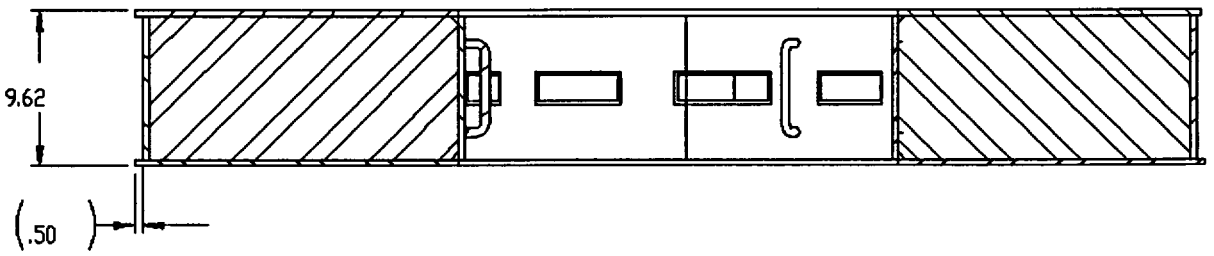

Elevation View Of Long Spacer

Figure P.4-18 Plan & Elevation Views of Short and Long Canister Spacers

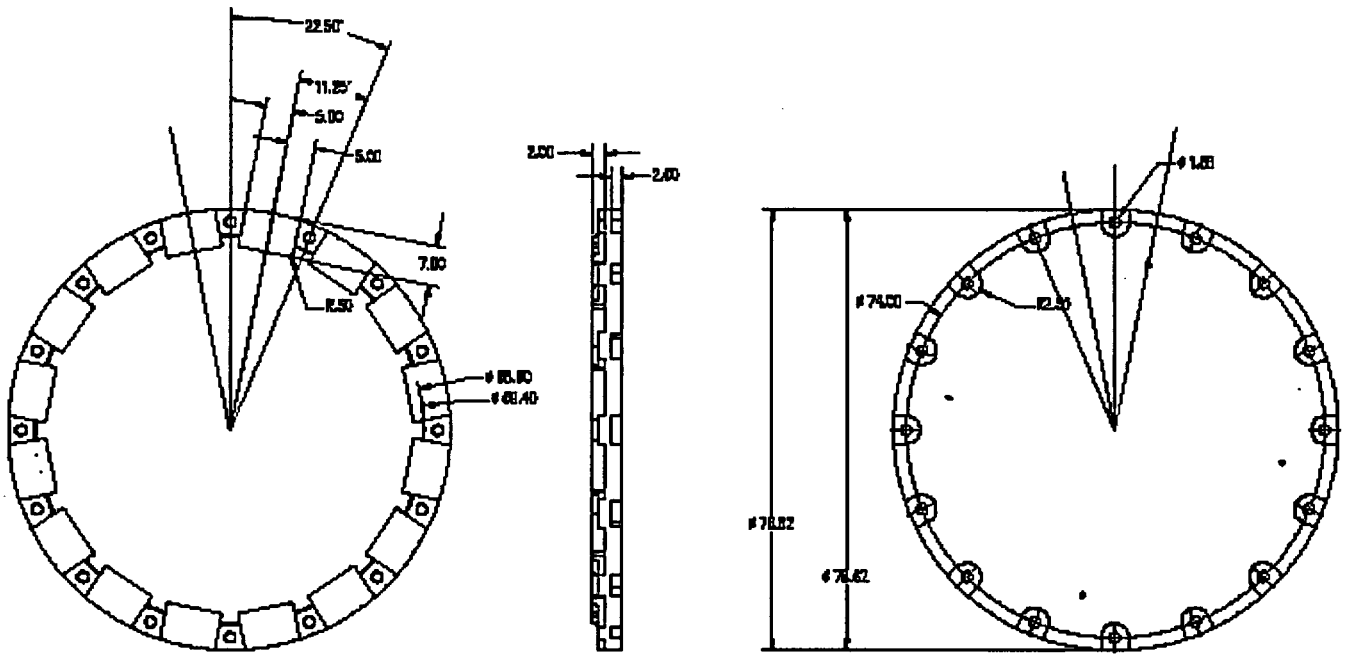

Figure P.4-19 OS197FC TC Lid With Slots For Air Exhaust

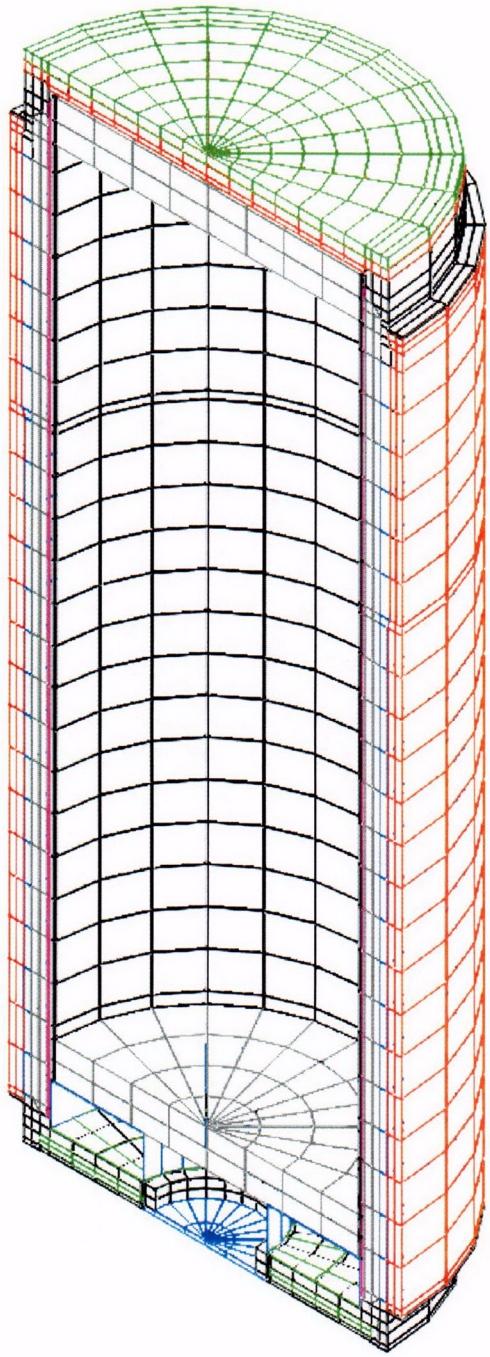

Figure P.4-20 Perspective View of OS197FC TC Assembly Thermal Model

C02

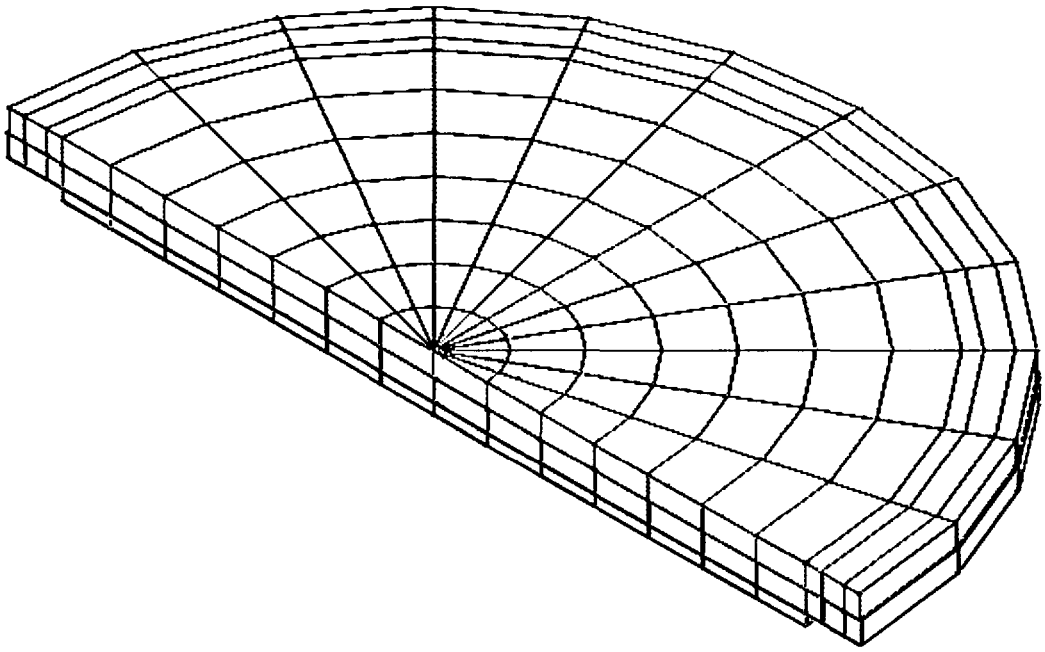

Perspective View of Thermal Model for Closure Lid & Cask Cover, Neutron Shield

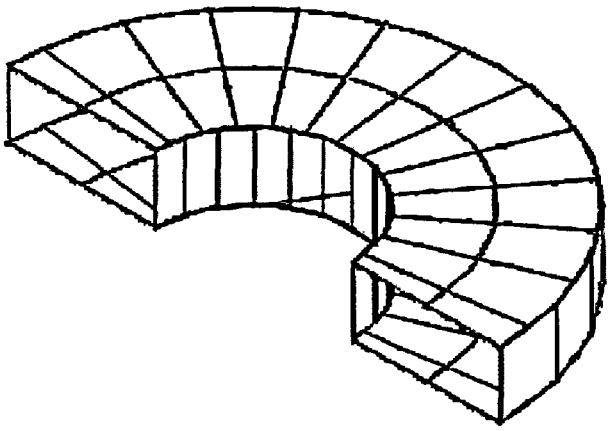

Perspective View of Thermal Model for Cask Spacer

Figure P.4-21 Perspective View of Thermal Model for Closure Lid, TC Cover, Neutron Shield, and TC Spacer

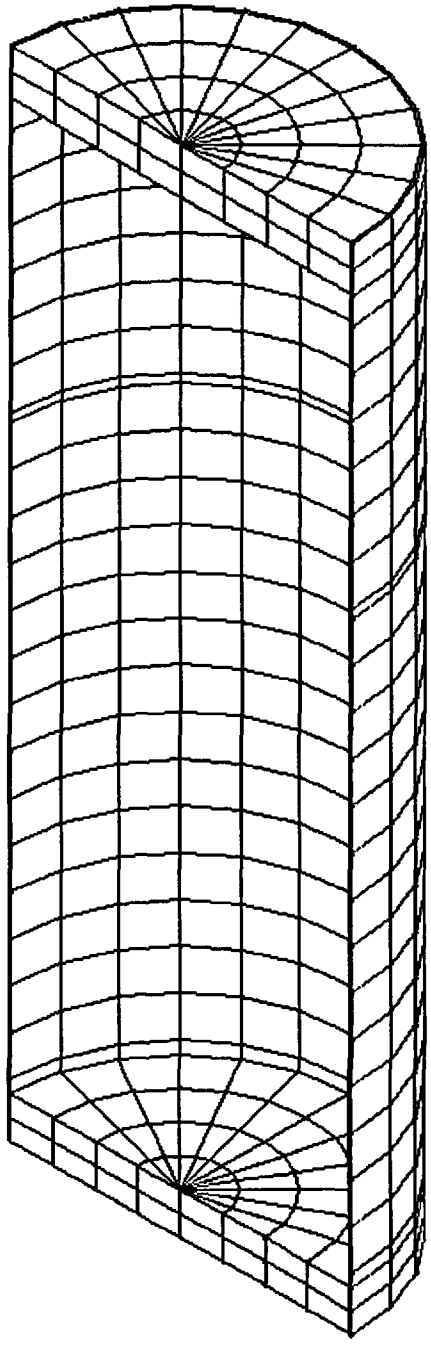

Figure P.4-22 Perspective View of Thermal Model For DSC Shell & Ends Used For Steady-State Analyses

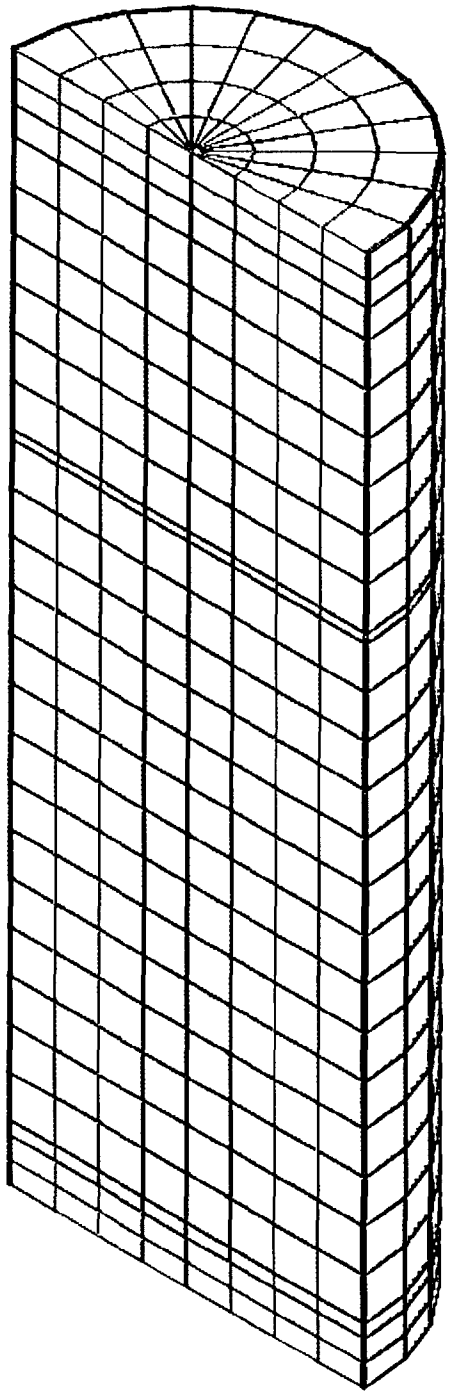

Figure P.4-23 Perspective View of Thermal Model For DSC Shell, Ends, & Basket Used For Transient Analyses in OS197FC TC

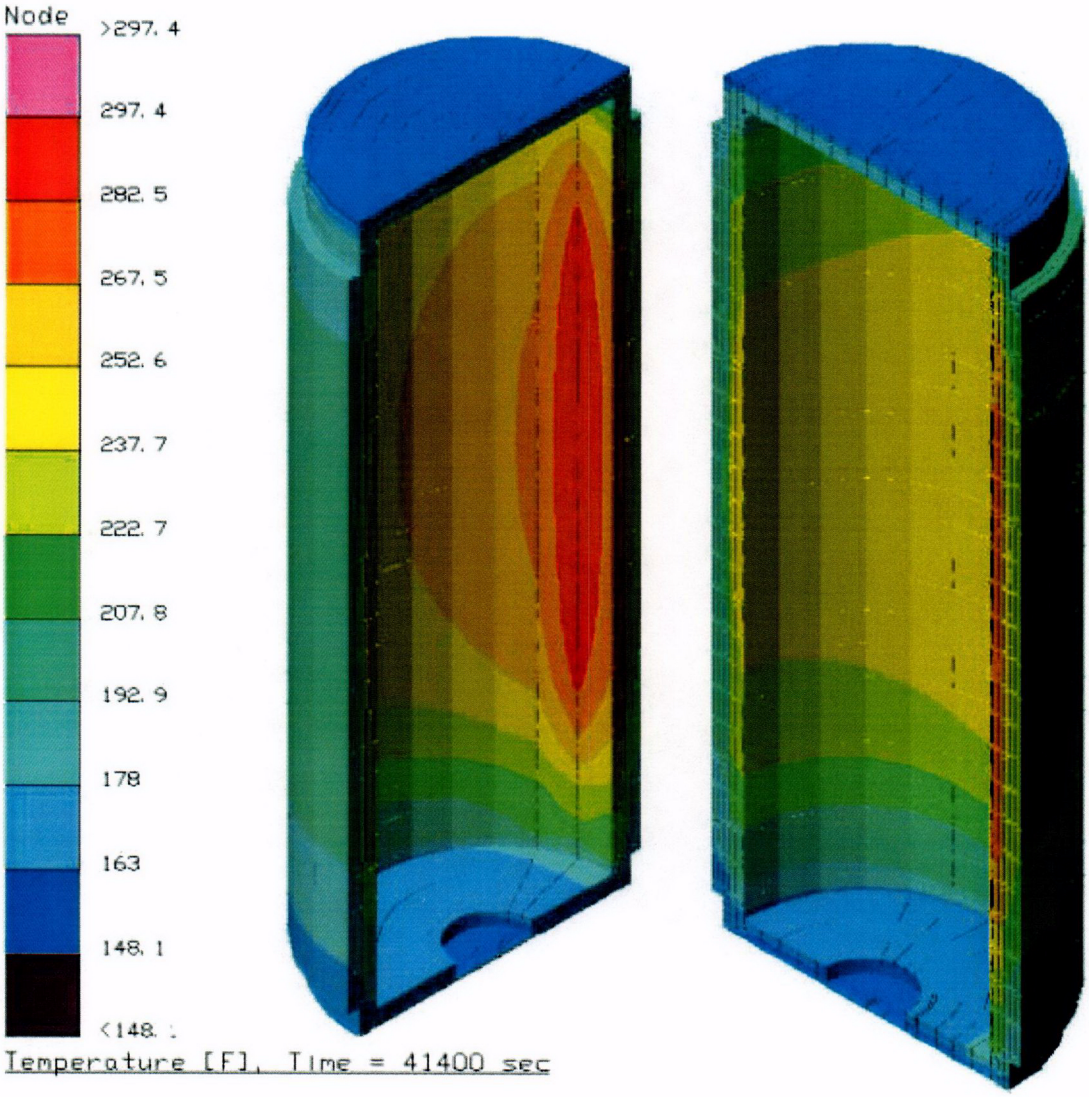

Figure P.4-24 Temperature Distribution at 11.5 hours for OS197FC TC during Transfer of 24PTH DSC, 40.8 kW Heat Load and 117°F Ambient

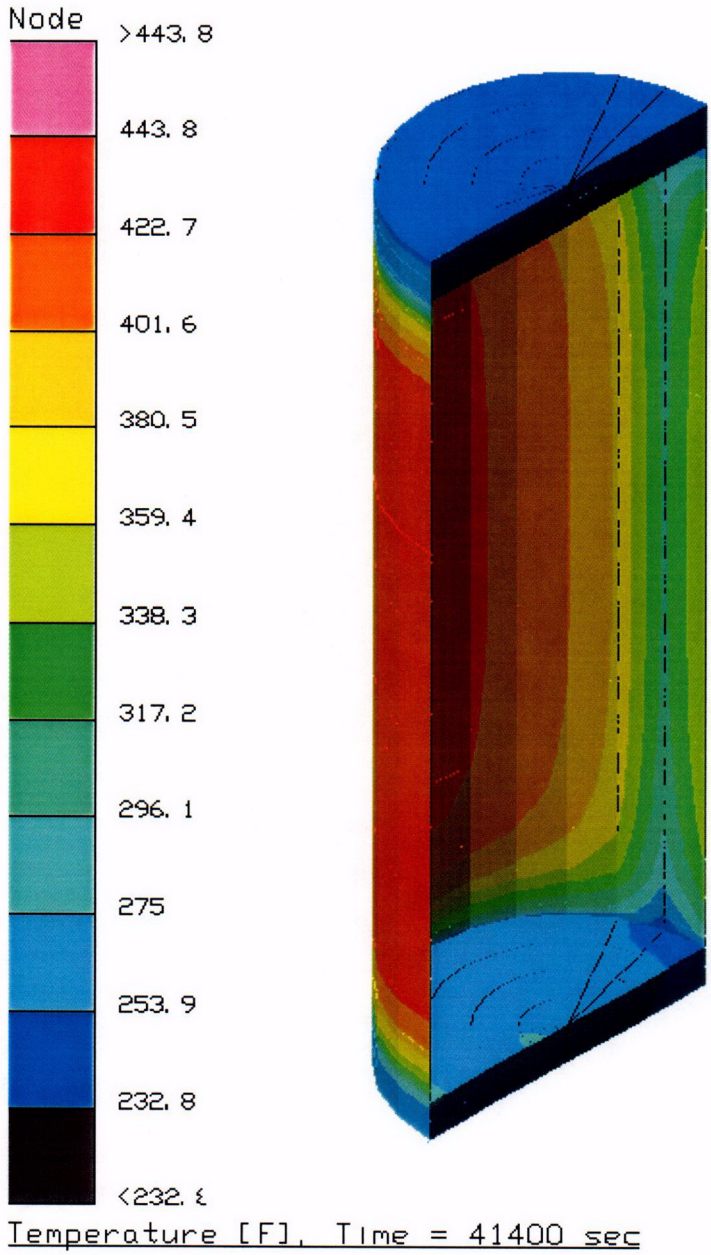

Figure P.4-25 Temperature Distribution at 11.5 hours for 24PTH DSC Shell Assembly during Transfer in OS197FC TC, 40.8 kW Heat Load and 117°F Ambient

C04

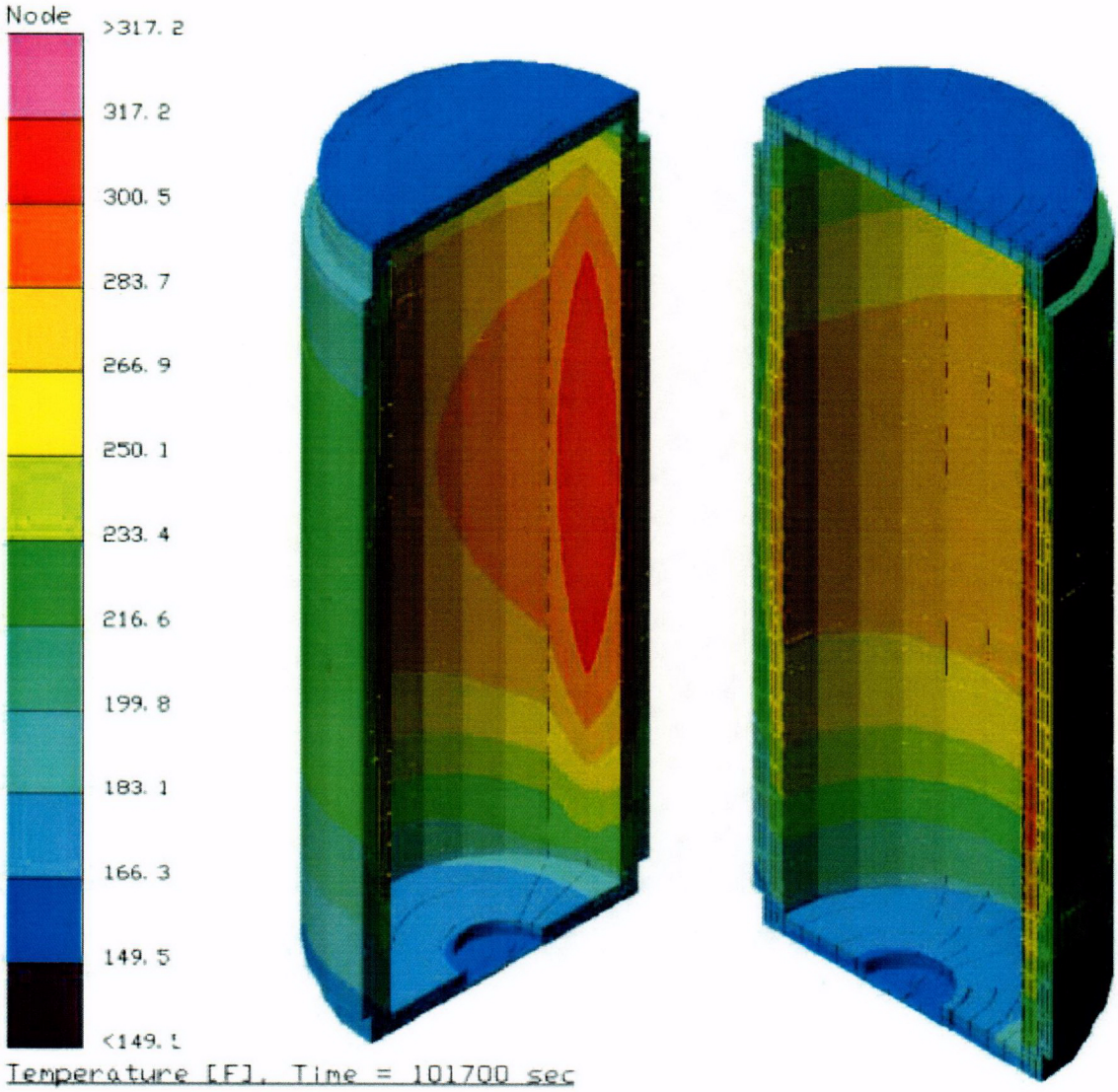

Figure P.4-26 Temperature Distribution at 28.3 hours for OS197FC TC during Transfer of 24PTH DSC, 31.2 kW Heat Load and 117°F Ambient

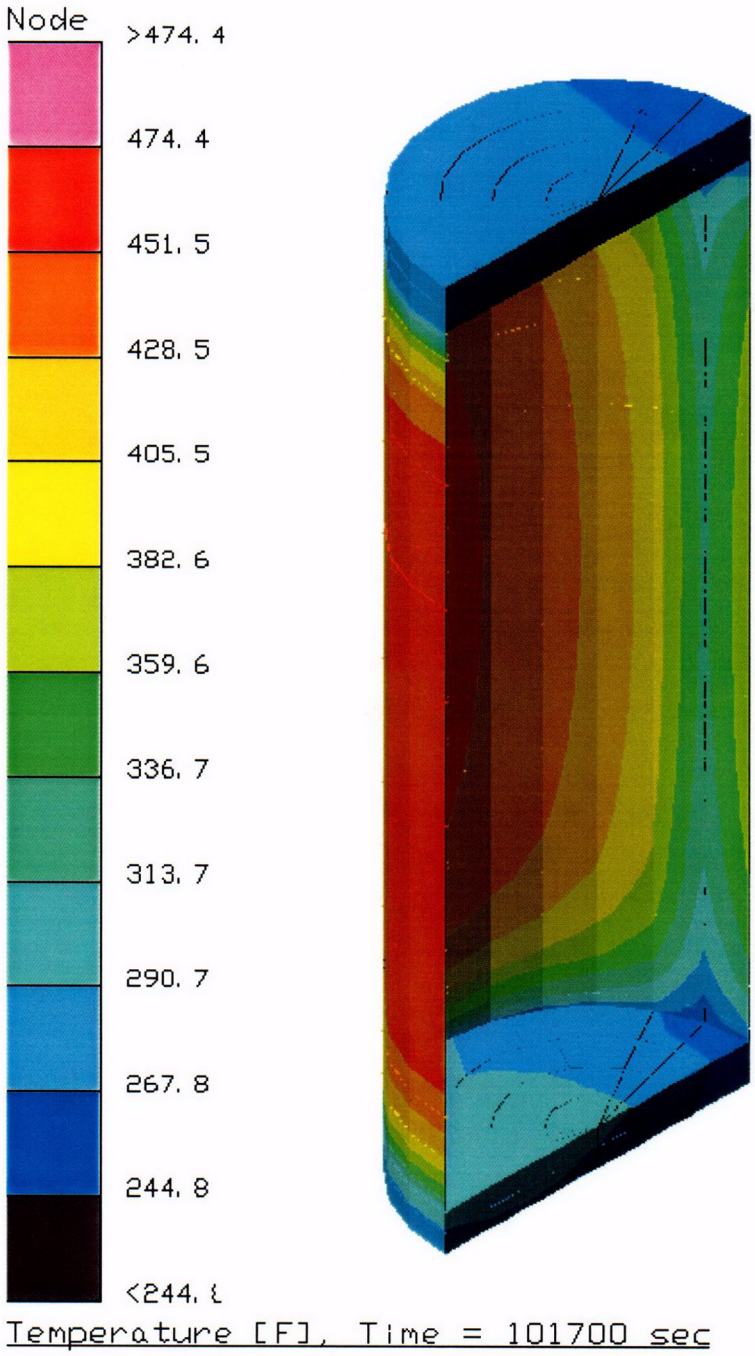

Figure P.4-27 Temperature Distribution at 28.3 hours for 24PTH DSC Shell Assembly during Transfer in OS197FC TC, 31.2 kW Heat Load and 117°F Ambient

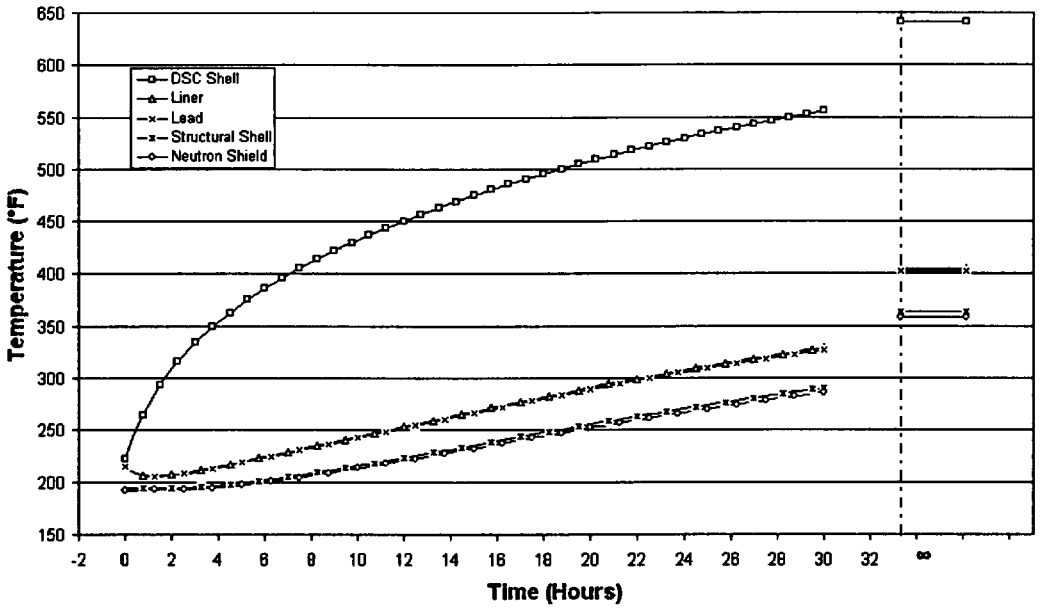

Figure P.4-28 Transient Temperature Response during Loading of 24PTH DSC with 40.8 kW into OS197FC TC, 100°F without Insolation (Cask Vertical)

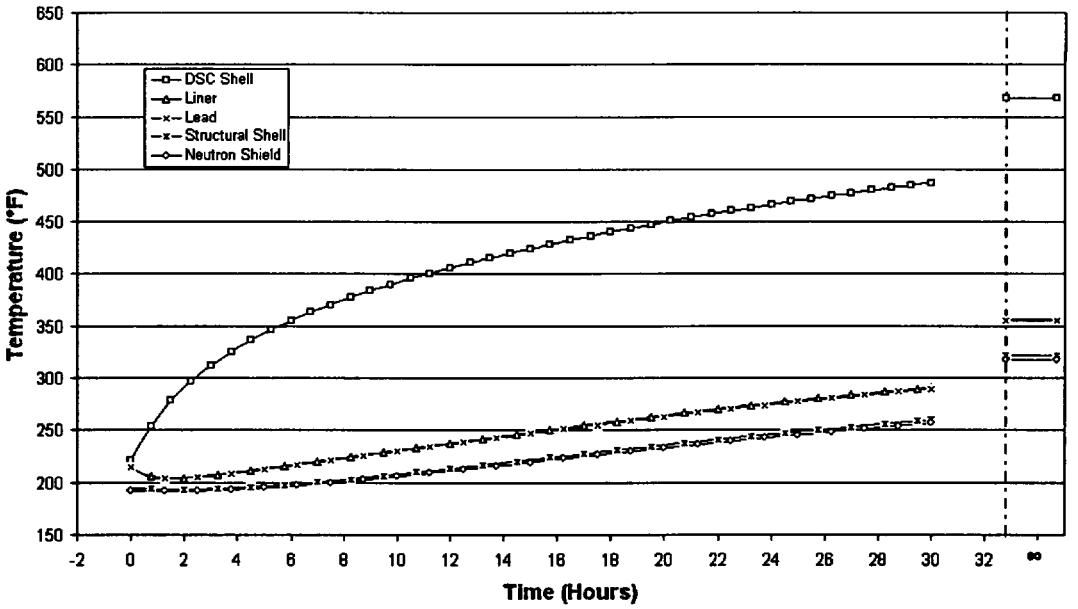

Figure P.4-29 Transient Temperature Response during Loading of 24PTH DSC with 31.2 kW into OS197FC TC, 100°F without Insolation (Cask Vertical)

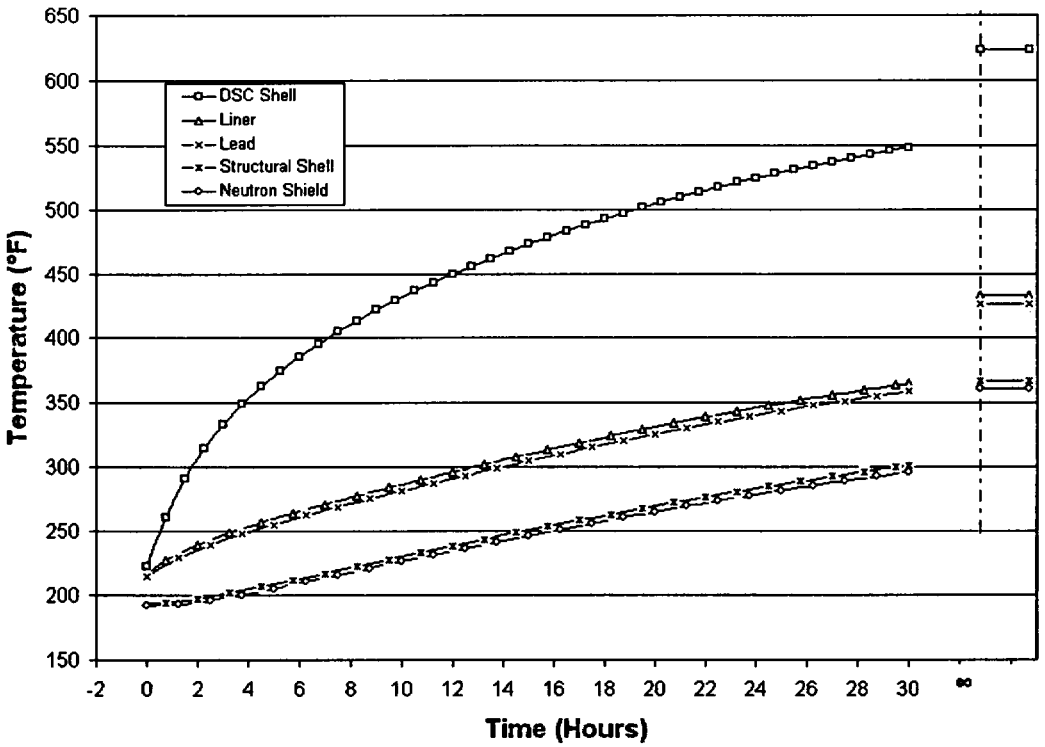

Figure P.4-30 Transient Temperature Response during Transfer of 24PTH DSC with 40.8 kW into OS197FC TC, 100°F with Insolation (Cask Horizontal)

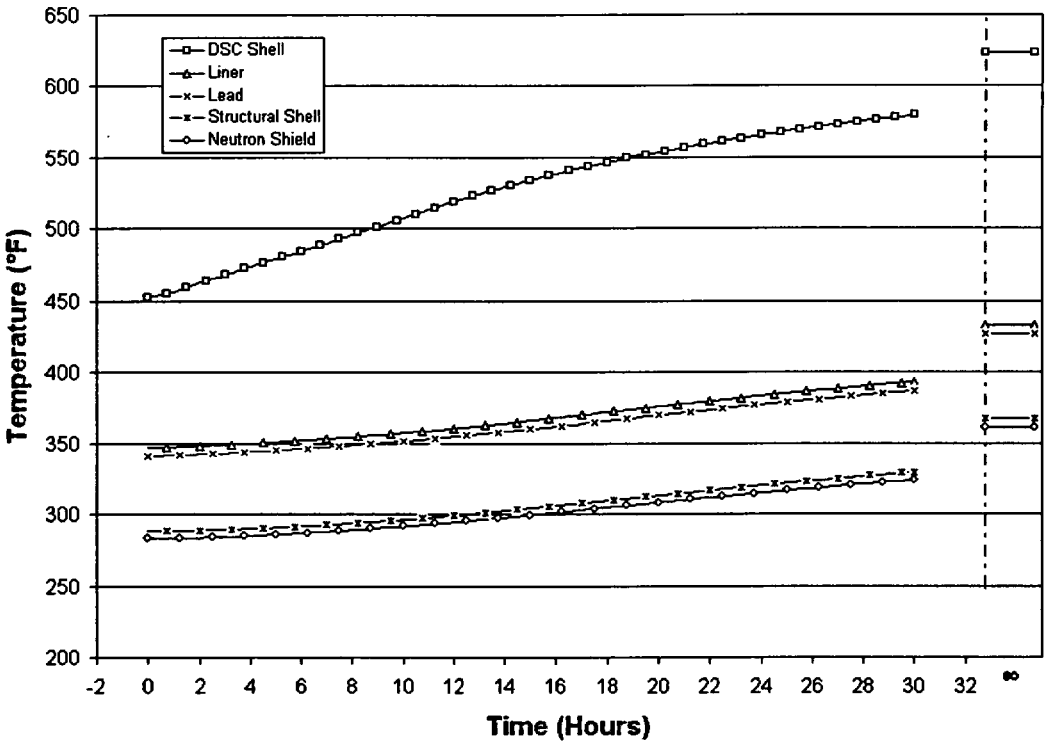

Figure P.4-31 Transient Temperature Response during Transfer of 24PTH DSC with 40.8 kW into OS197FC TC and Loss of Air Circulation Accident (Cask Horizontal)

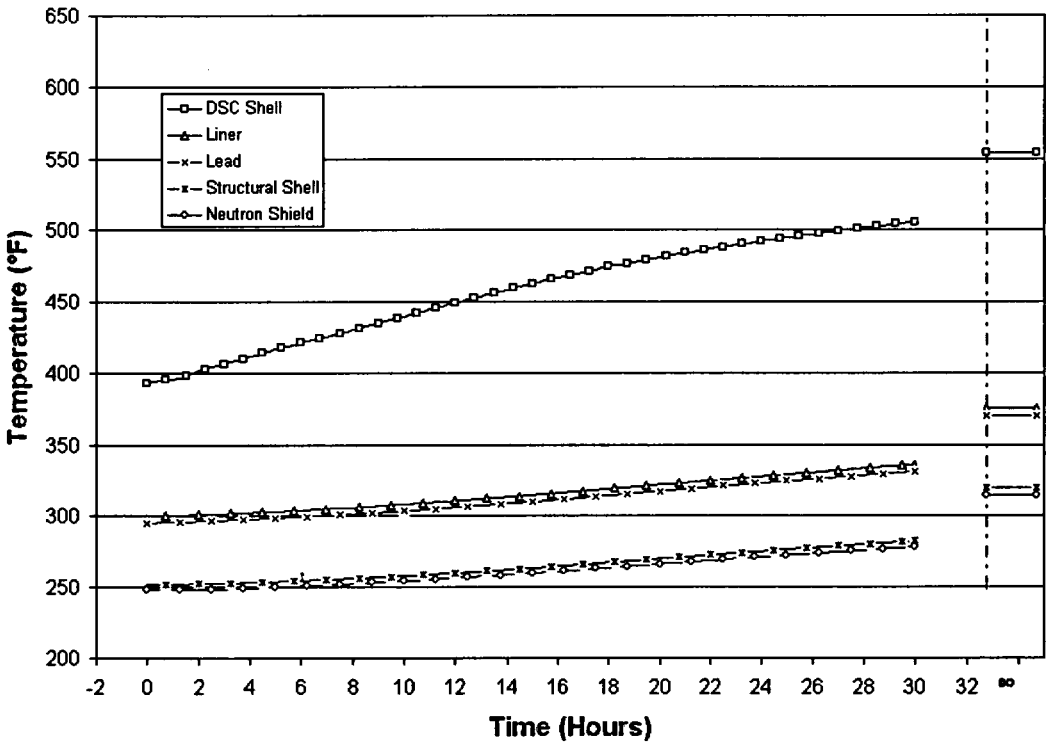

Figure P.4-32 Transient Temperature Response during Transfer of 24PTH DSC with 31.2 kW into OS197FC TC and Loss of Air Circulation Accident (Cask Horizontal)

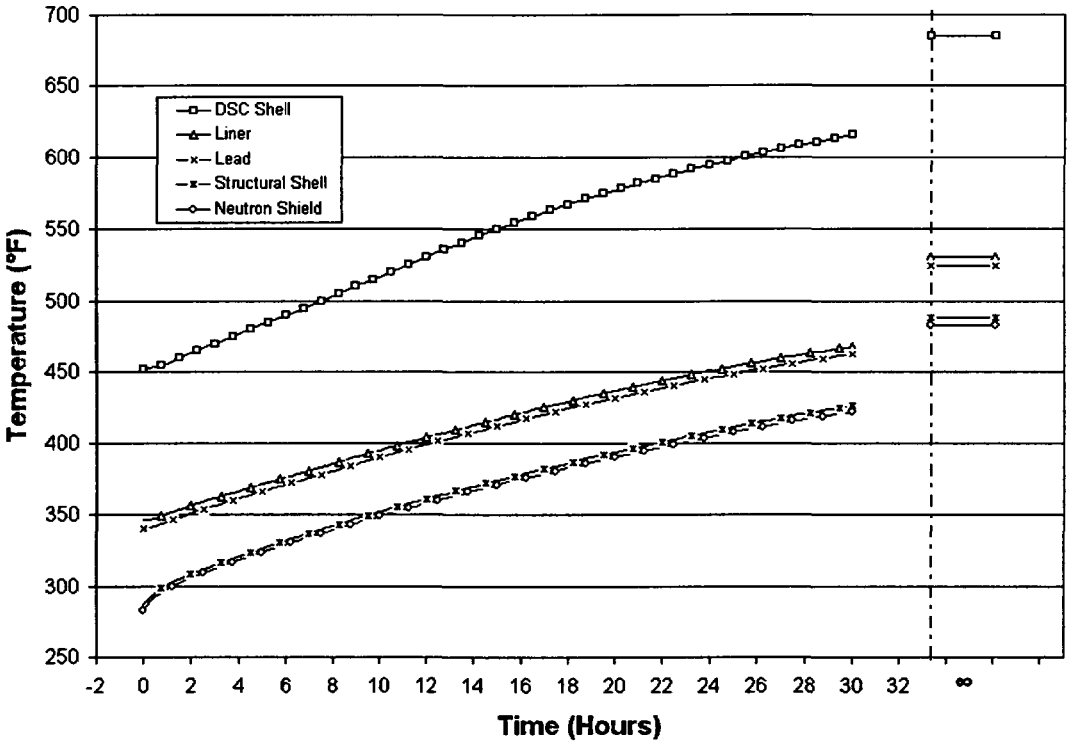

Figure P.4-33 Loss of Neutron Shield and Air Circulation (if used) Accident Transient Temperature Response with 40.8 kW (Cask Horizontal)

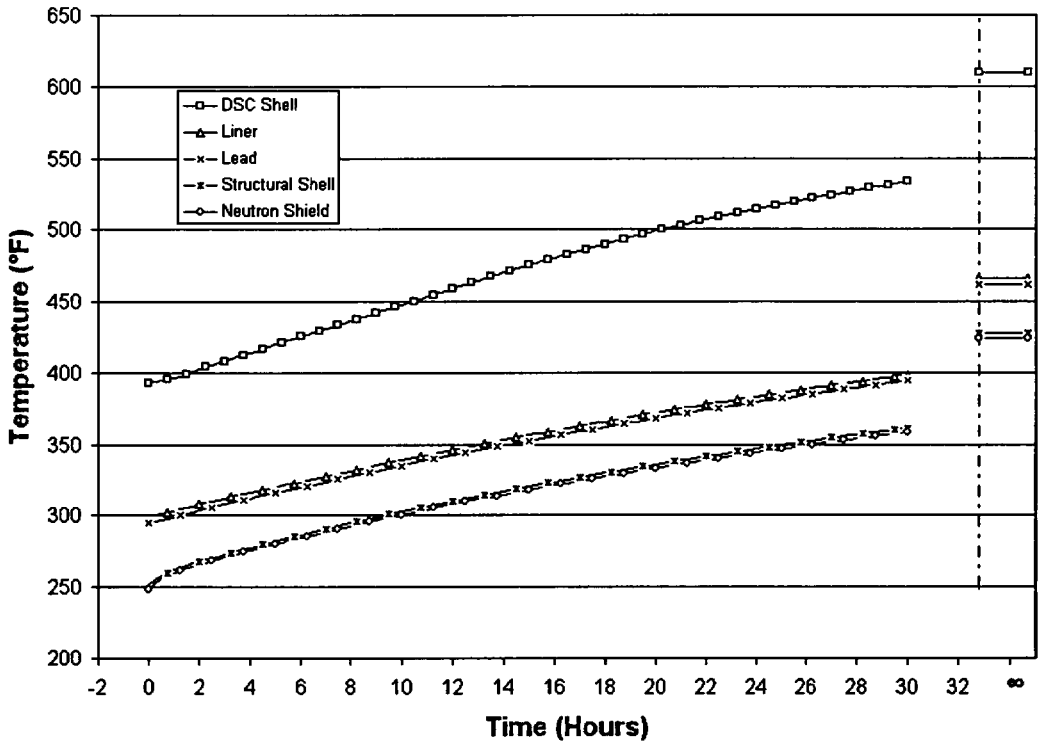

Figure P.4-34 Loss of Neutron Shield and Air Circulation (if used) Accident Transient Temperature Response with 31.2 kW (Cask Horizontal)

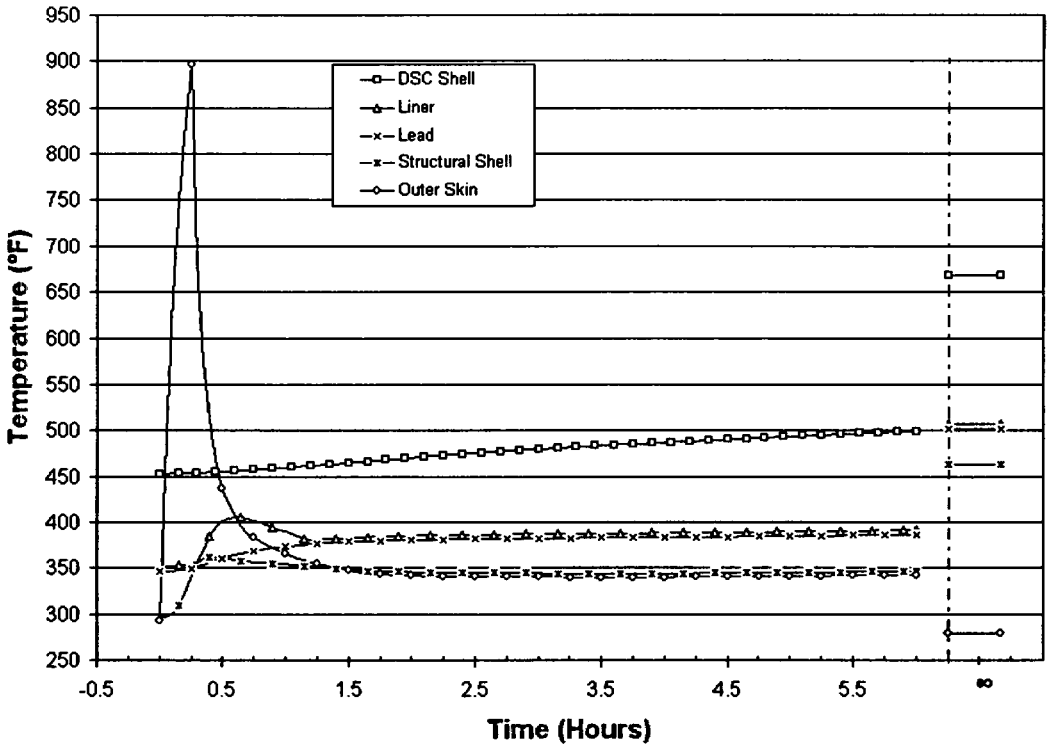

Figure P.4-35 24PTH DSC in OS197FC TC Fire Accident Transient Response with 40.8 kW

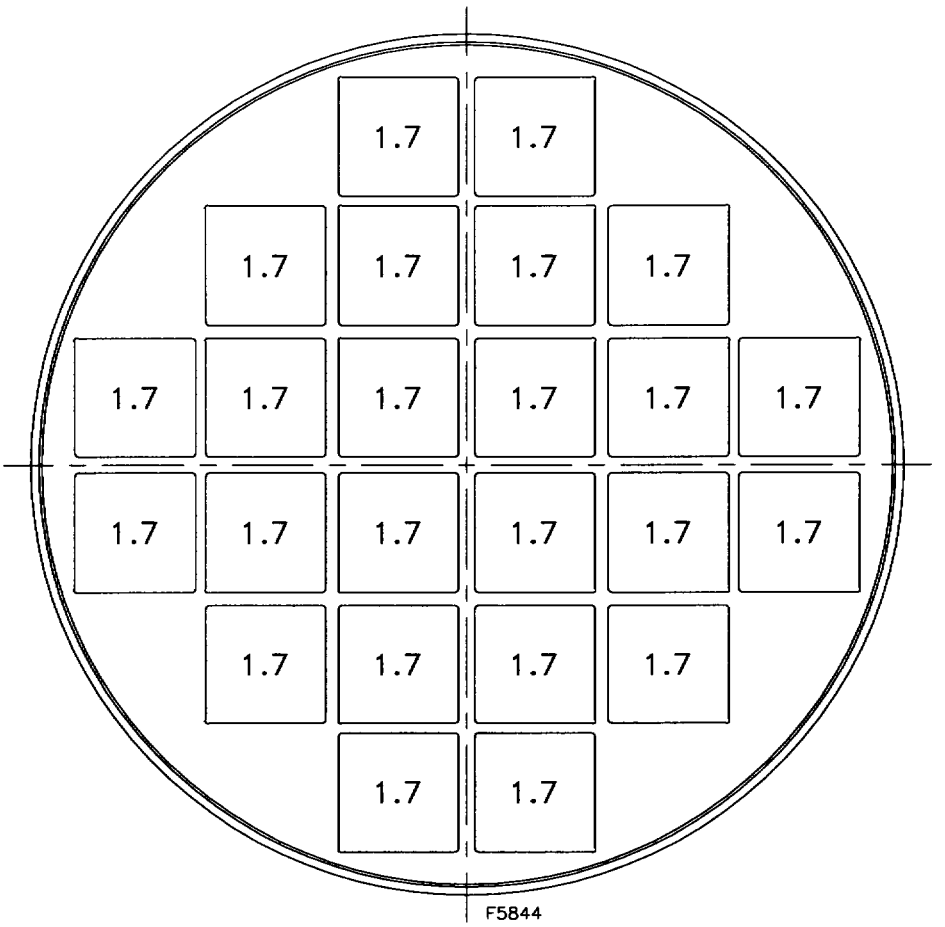

Figure P.4-36 24PTH-S and 24PTH-L DSC, HLZC 1, 40.8 kW Maximum Decay Heat

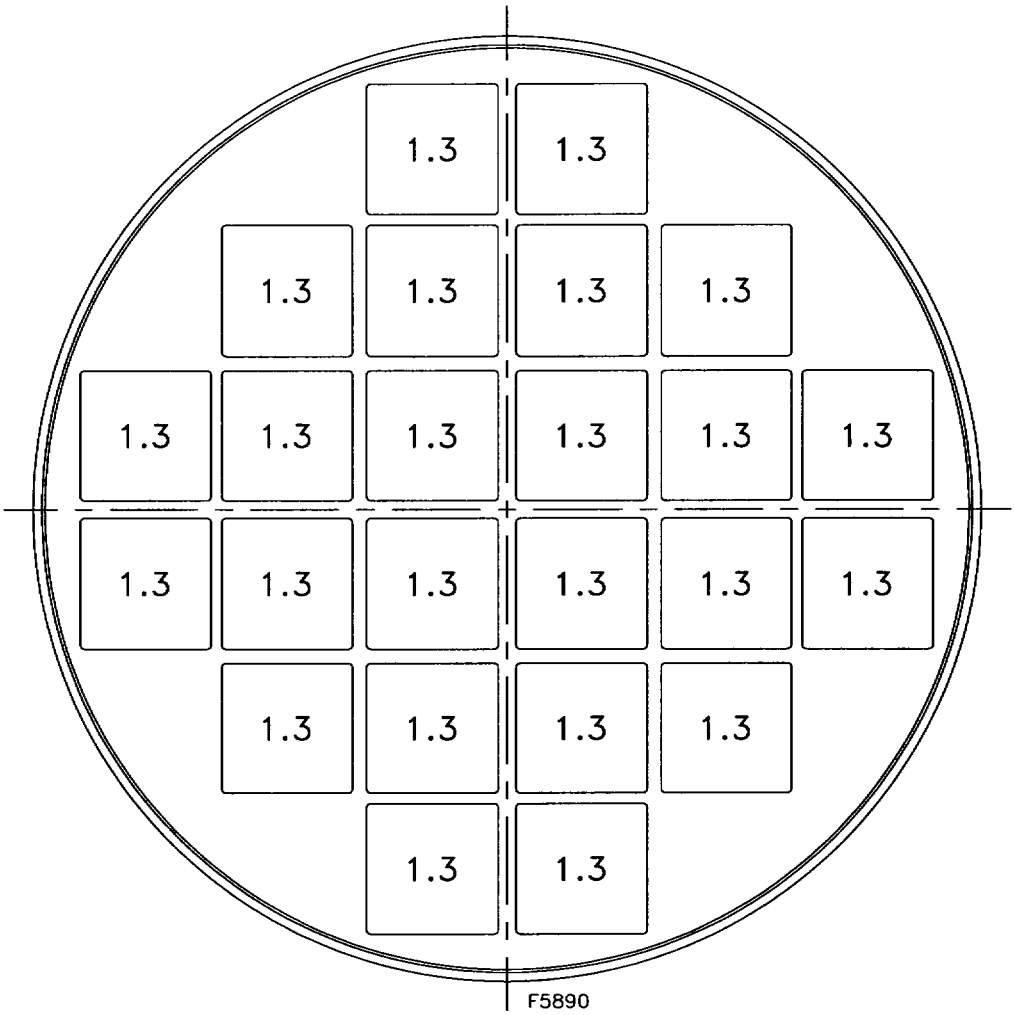

Figure P.4-37 24PTH-S and 24PTH-L DSC HLZC 4, 31.2 kW Maximum Decay Heat

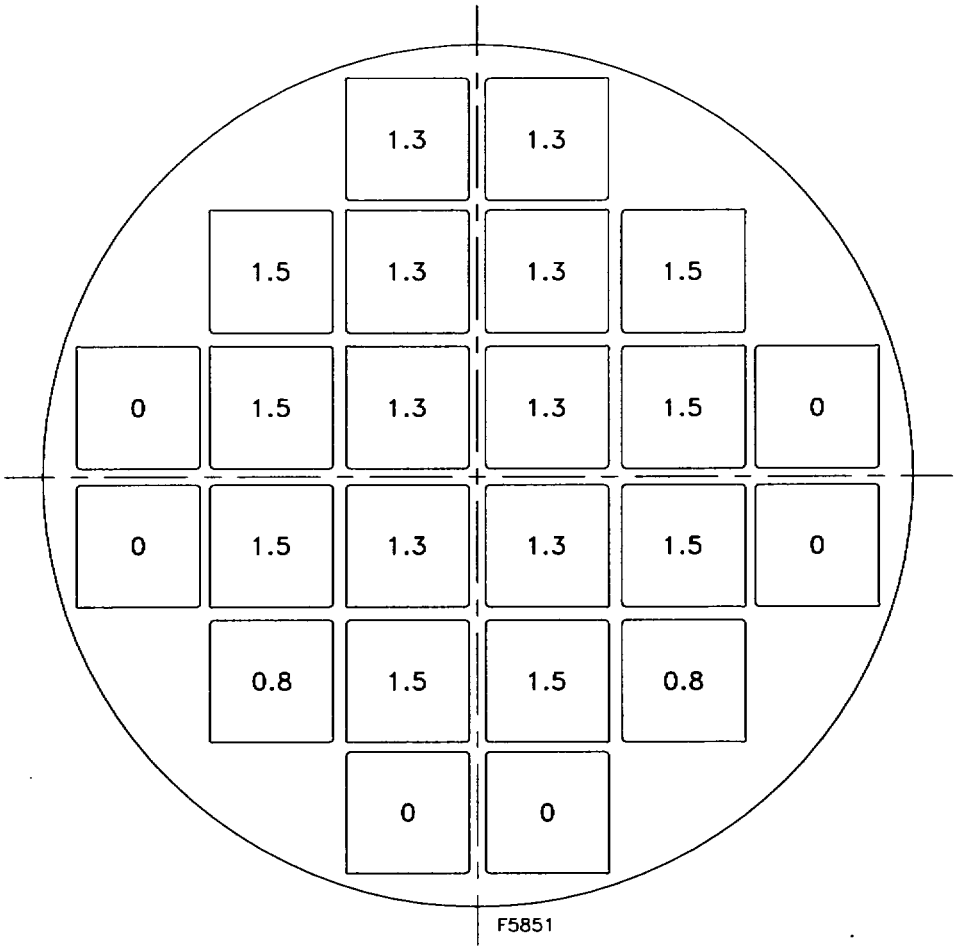

Figure P.4-38 24PTH-S-LC DSC HLZC 5, 24 kW Maximum Decay Heat

The "zero" cells could have heat load of up to 1.5 kW per assembly (subject to a maximum heat load of 24 kW per DSC)

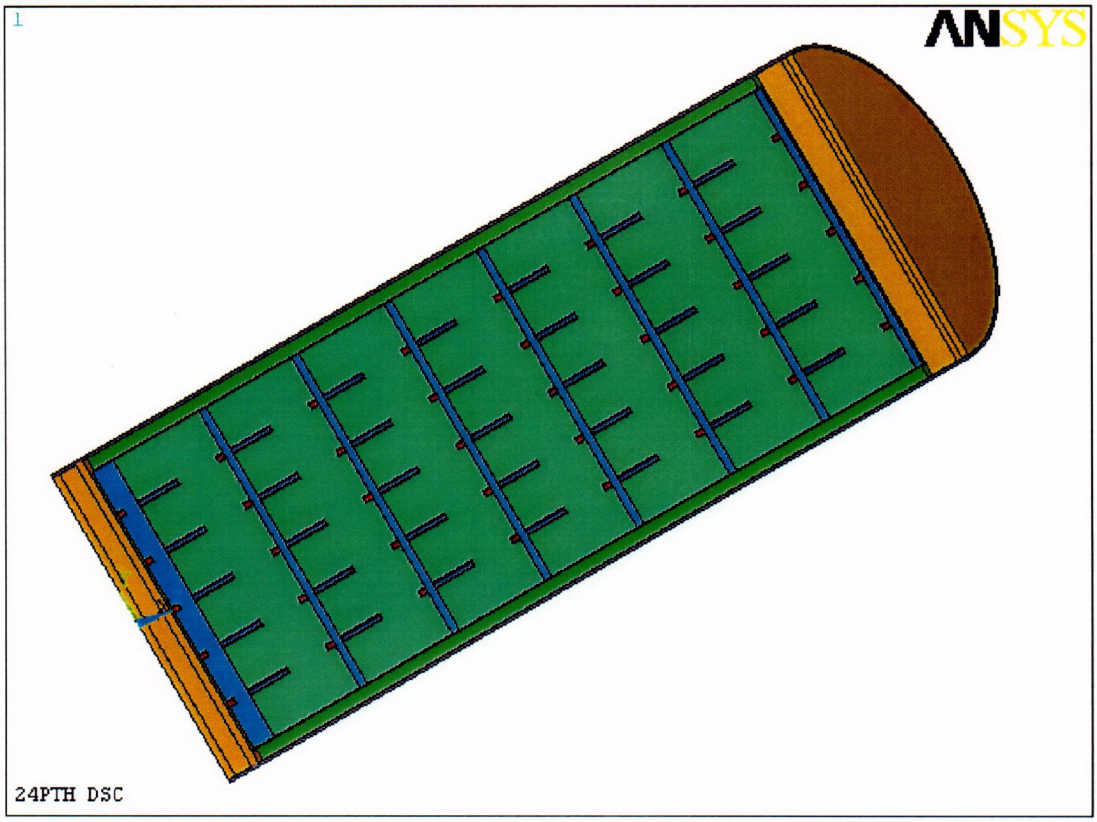

Figure P.4-39 24PTH DSC Thermal ANSYS Model

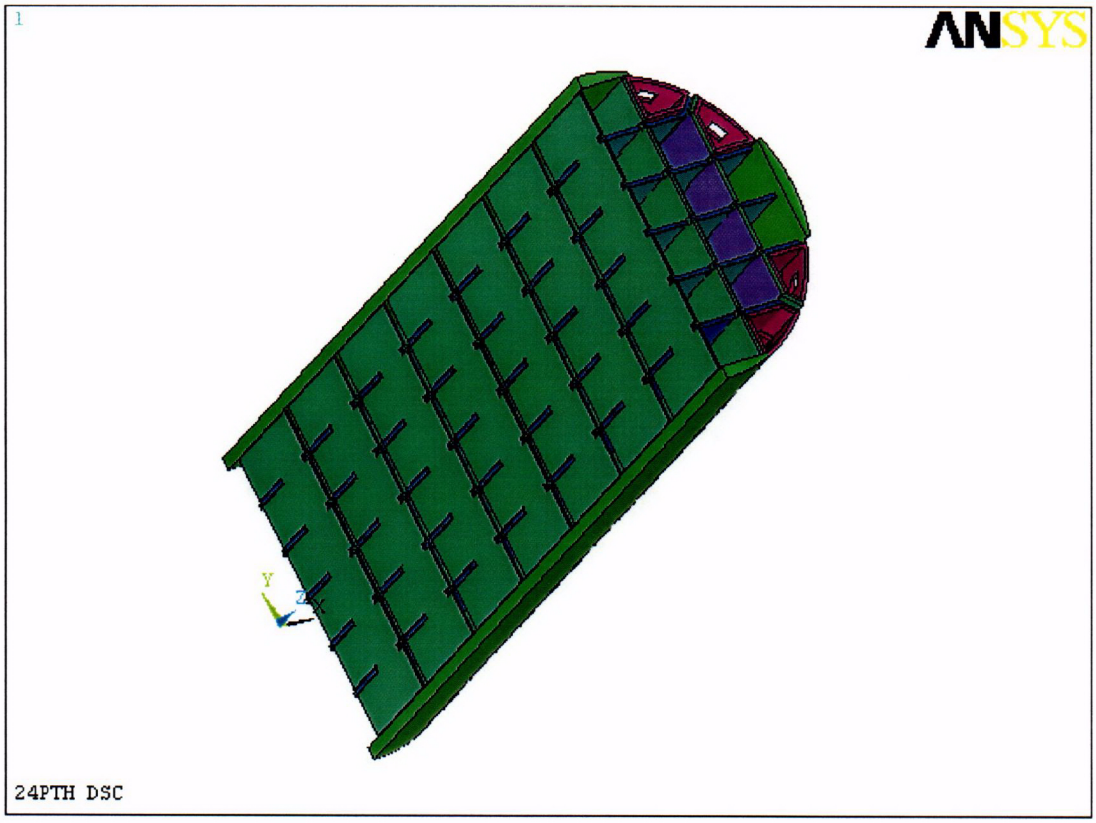

Figure P.4-40 24PTH DSC Thermal ANSYS Model, Basket Components

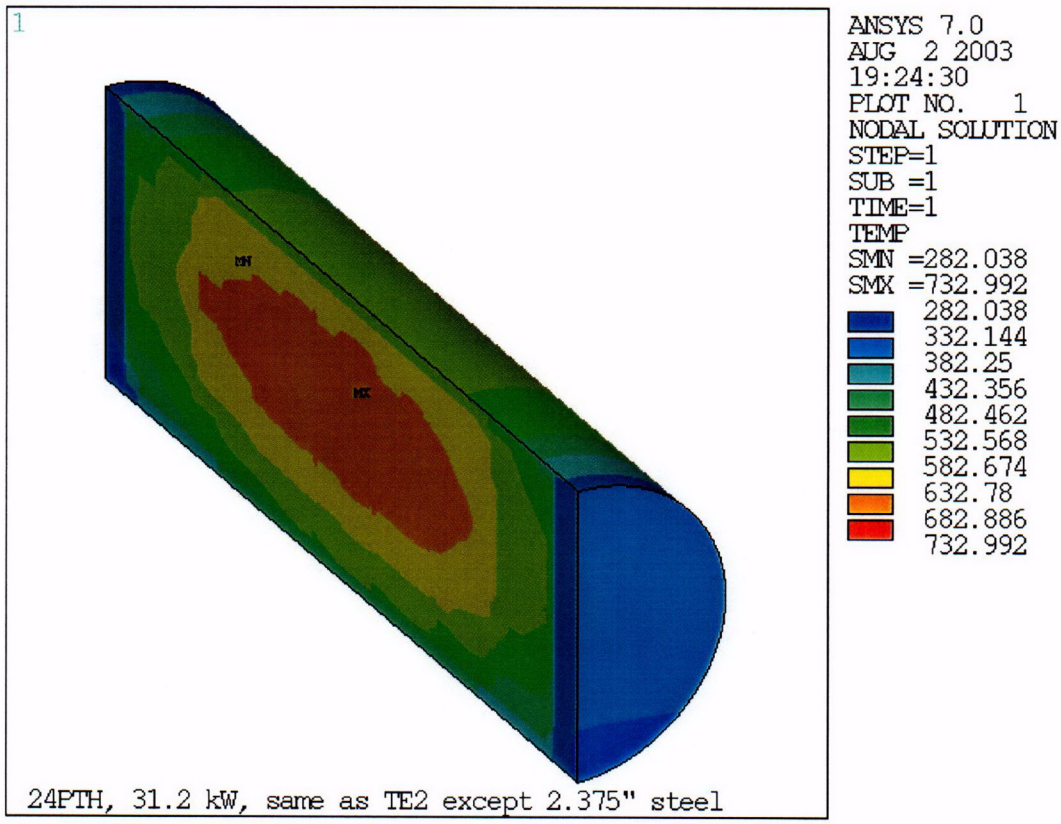

Figure P.4-41 Temperature Distribution in 24PTH DSC for 100°F Transfer Case with HLZC 4

C09

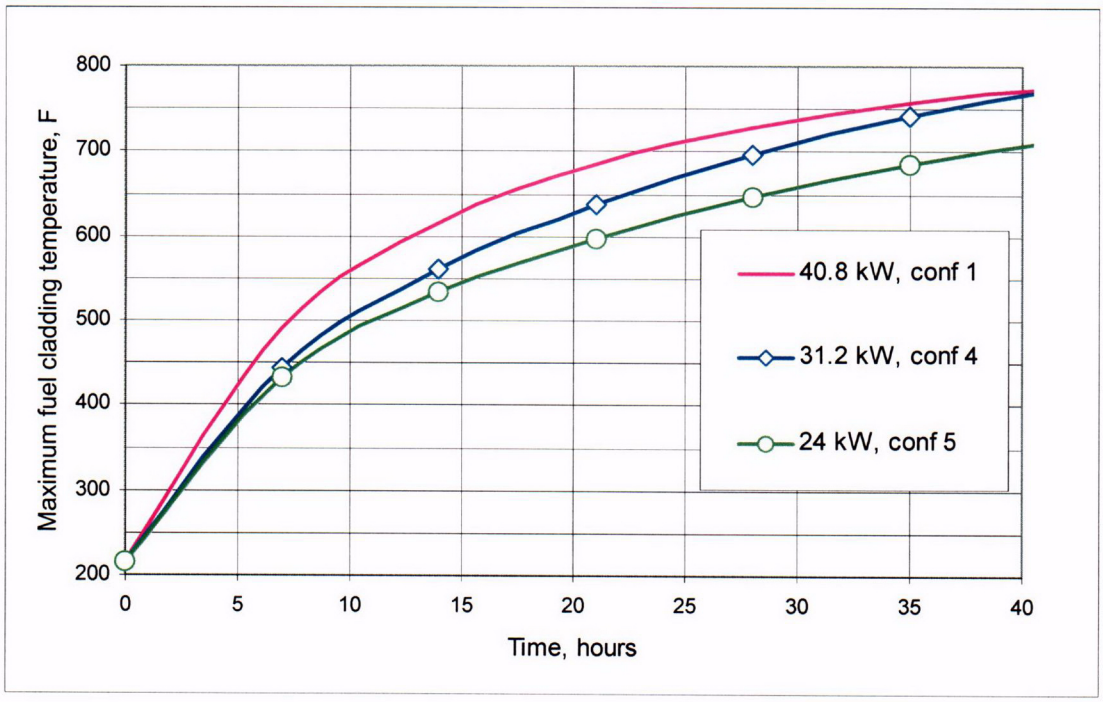

Figure P.4-42 Maximum Fuel Temperatures during Vacuum Drying Transient with Air for HLZCs 1, 4, and 5

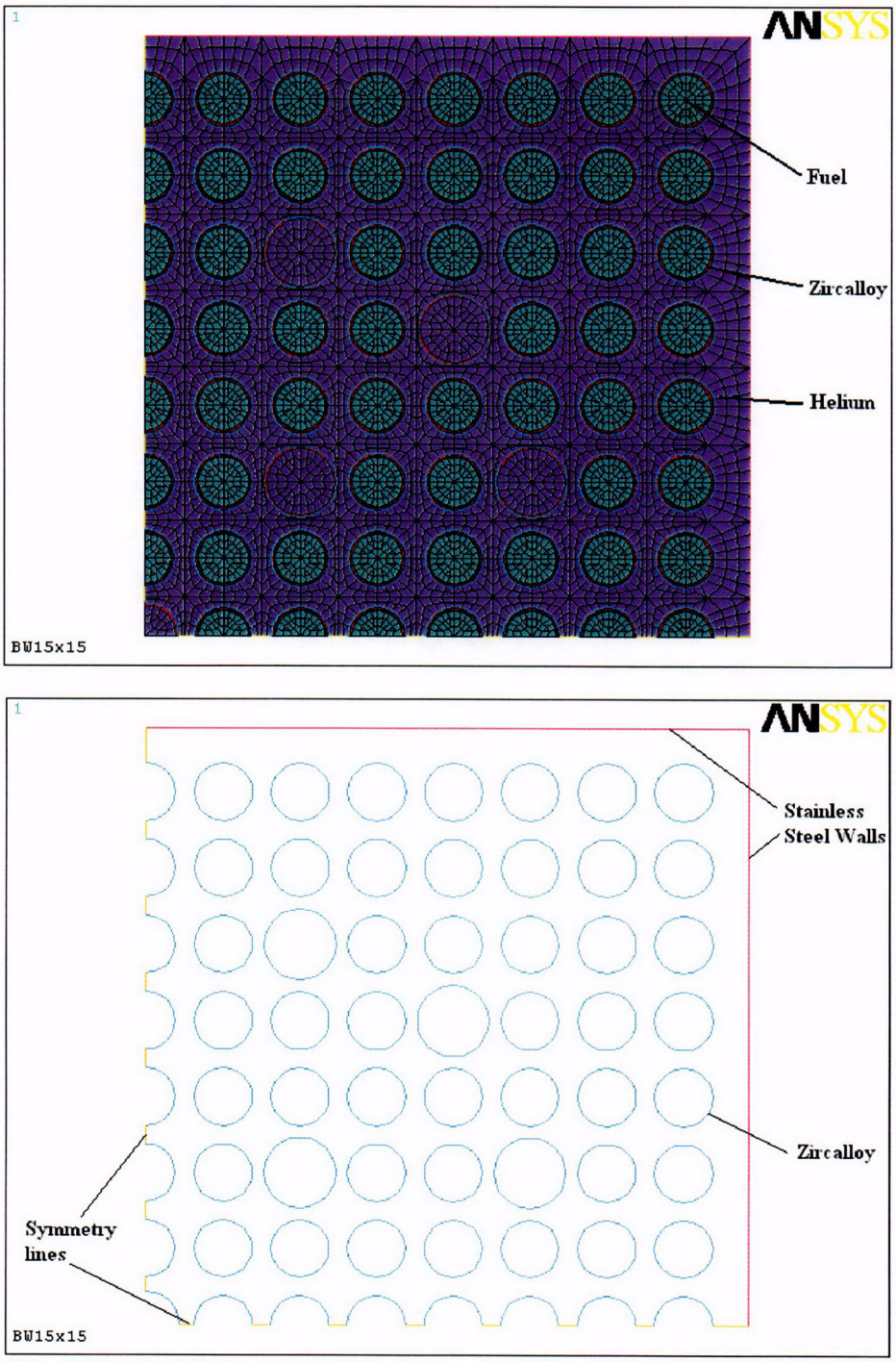

Figure P.4-43 Finite Element Model of B&W 15x15 Fuel Assembly

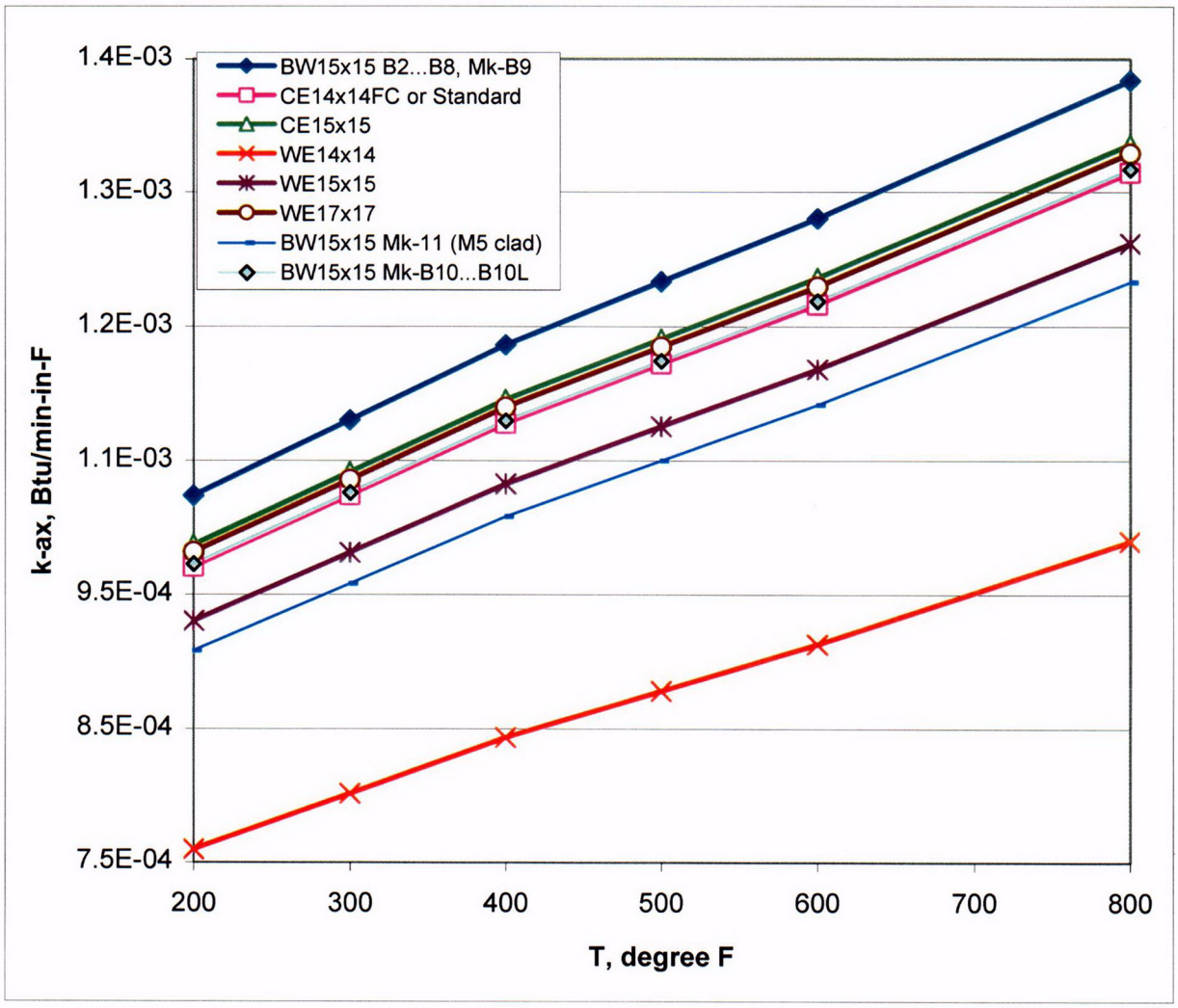

Figure P.4-44 Axial Fuel Effective Thermal Conductivity, All Fuels

C12

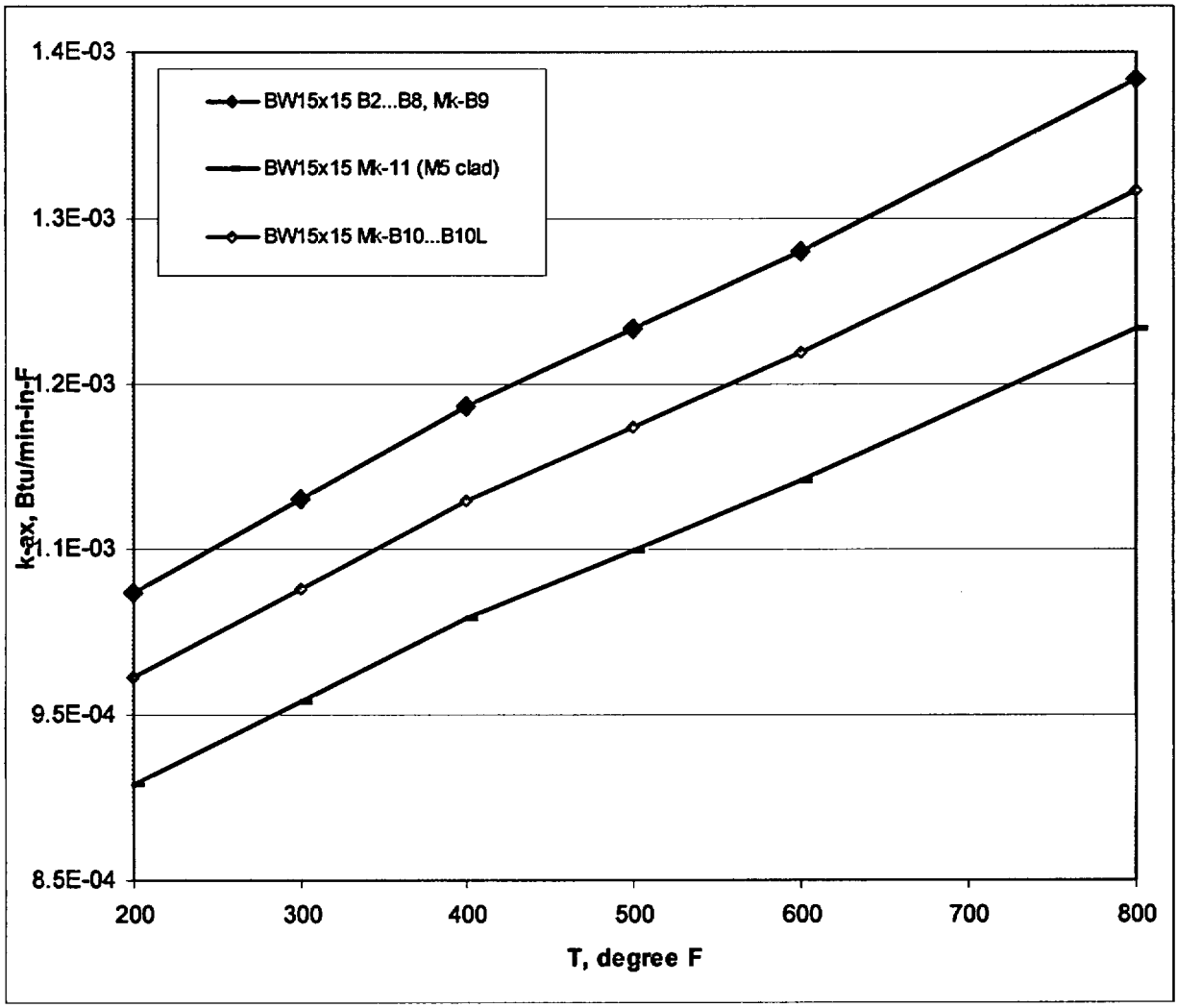

Figure P.4-45 Axial Fuel Effective Thermal Conductivity, B&W 15x15 Fuel Types

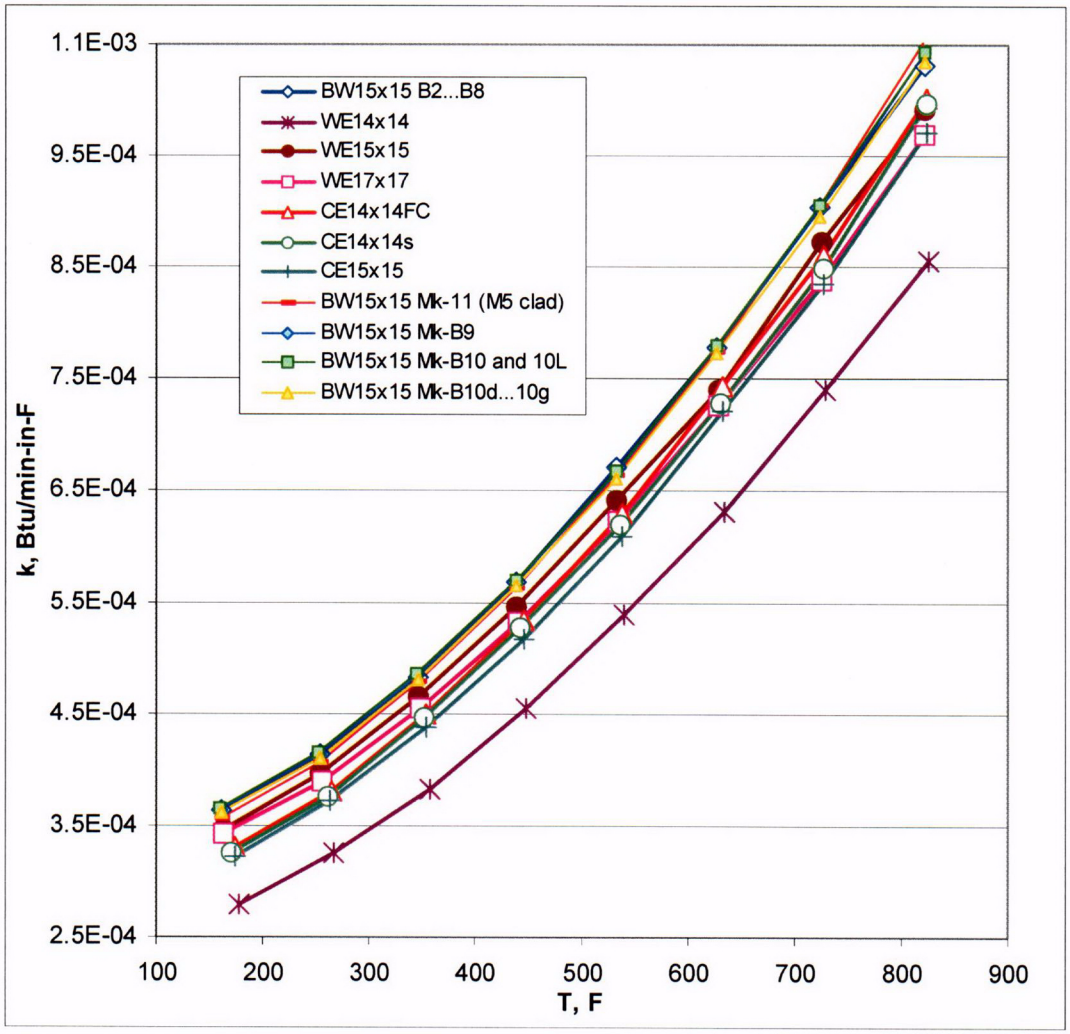

Figure P.4-46 Fuel Transverse Effective Thermal Conductivity in Helium, All Fuels

C13

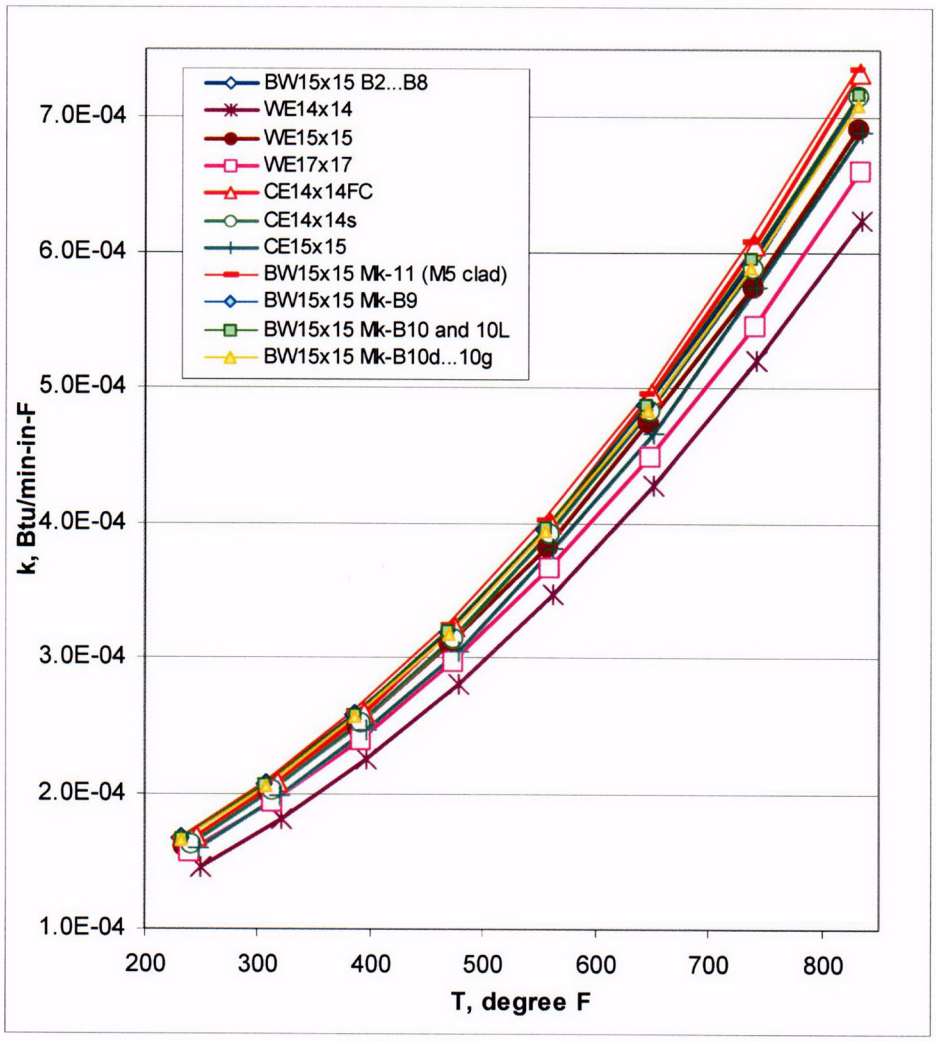

Figure P.4-47 Fuel Transverse Effective Thermal Conductivity in Vacuum, All Fuels

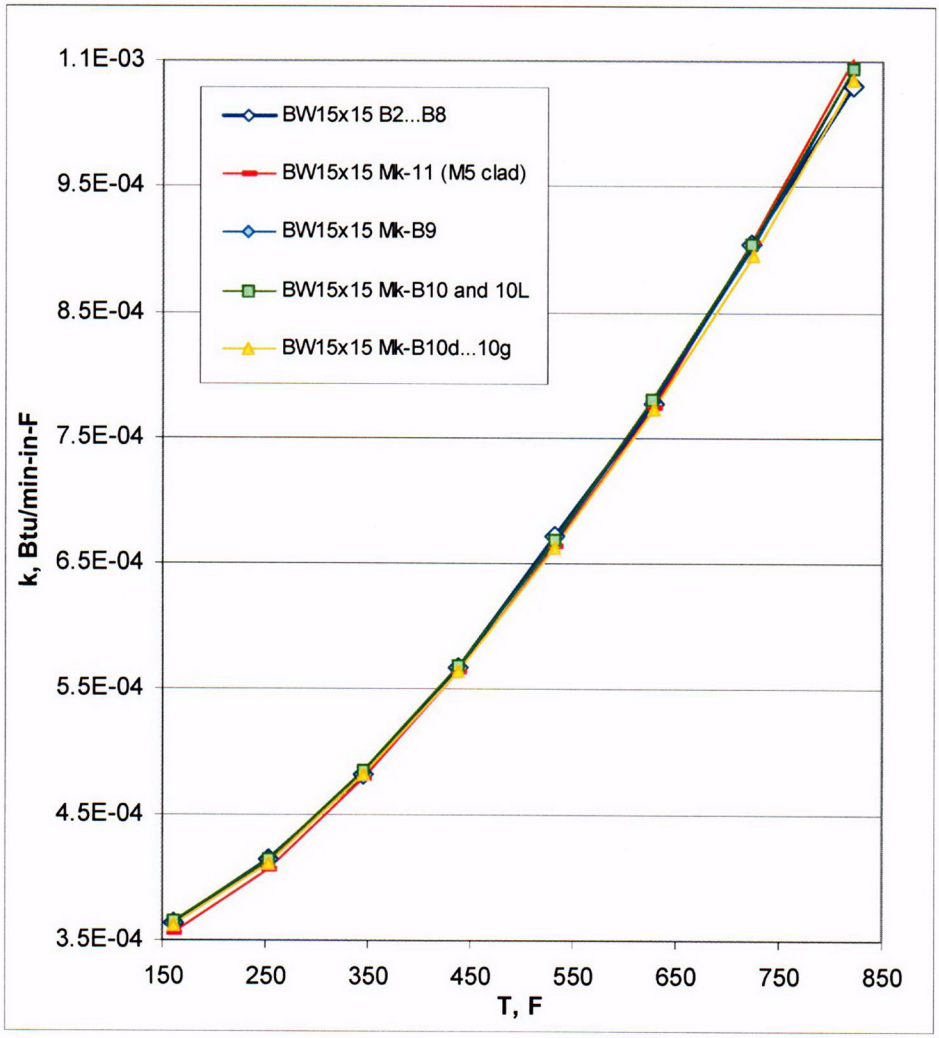

Figure P.4-48 Fuel Transverse Effective Thermal Conductivity in Helium, B&W 15x15 Fuels

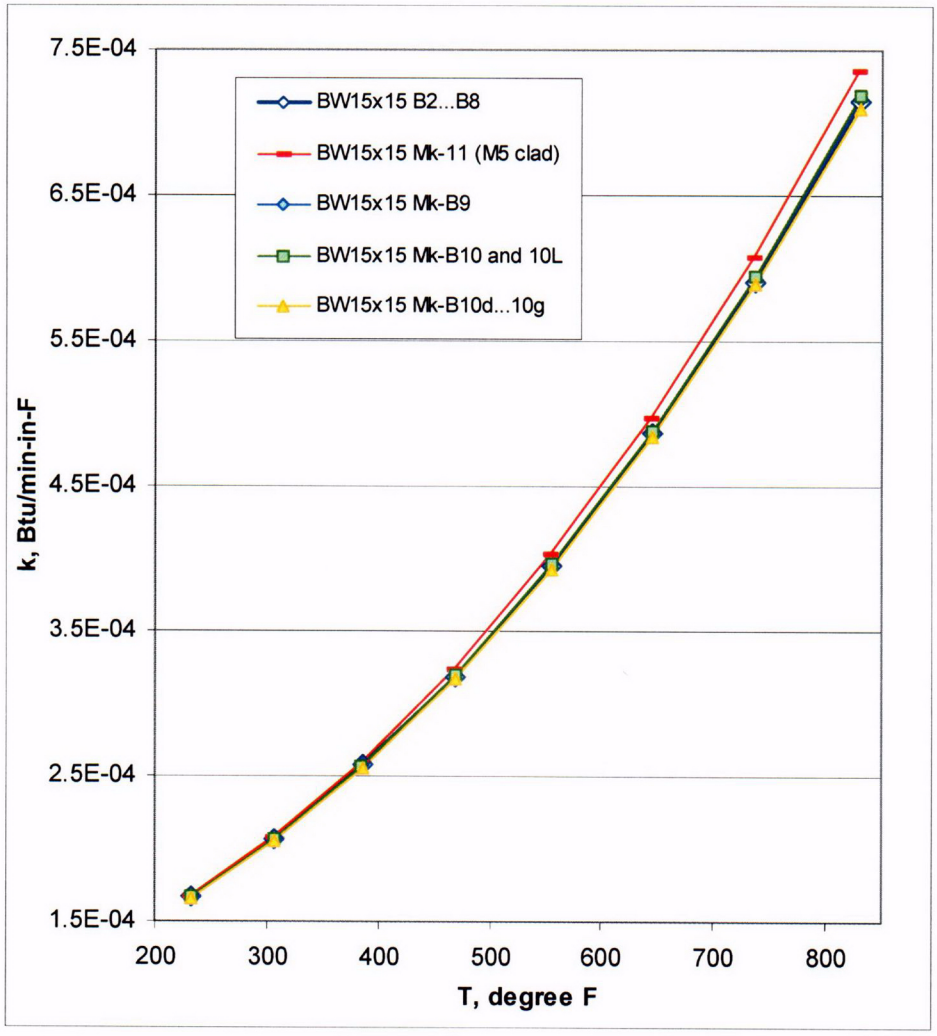

Figure P.4-49 Fuel Transverse Effective Thermal Conductivity in Vacuum, B&W 15x15 Fuels

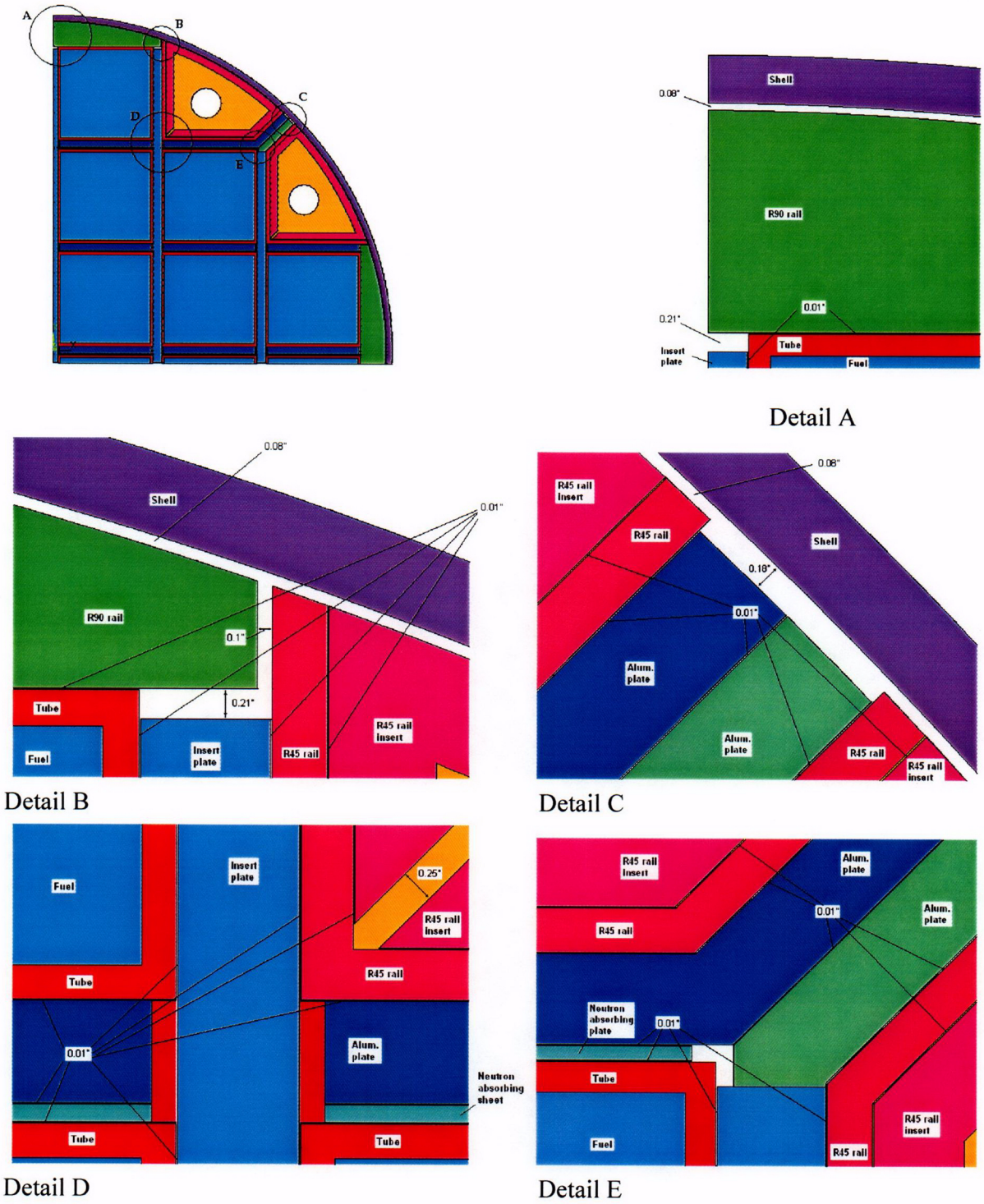

Figure P.4-50 Gaps Used in the 24PTH DSC ANSYS Model

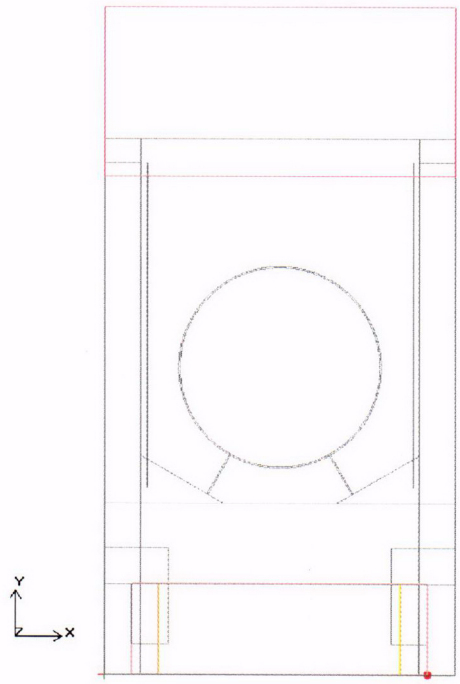

Figure P.4-51 Elevation View Of Model Layout

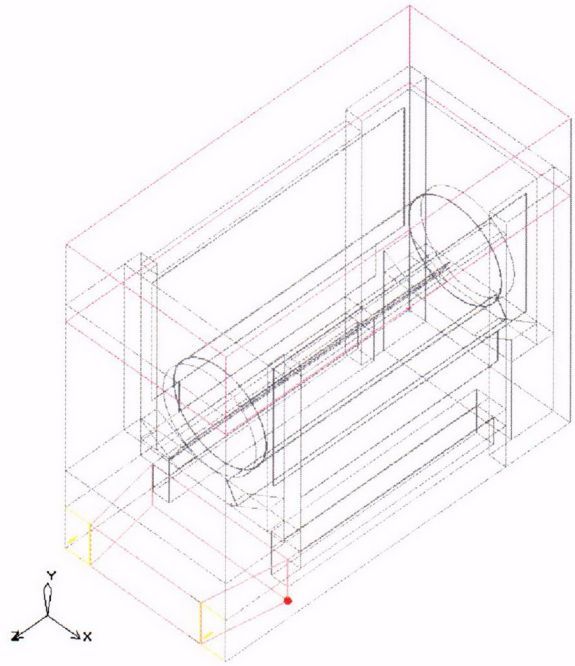

Figure P.4-52 Isometric View Of Model Layout

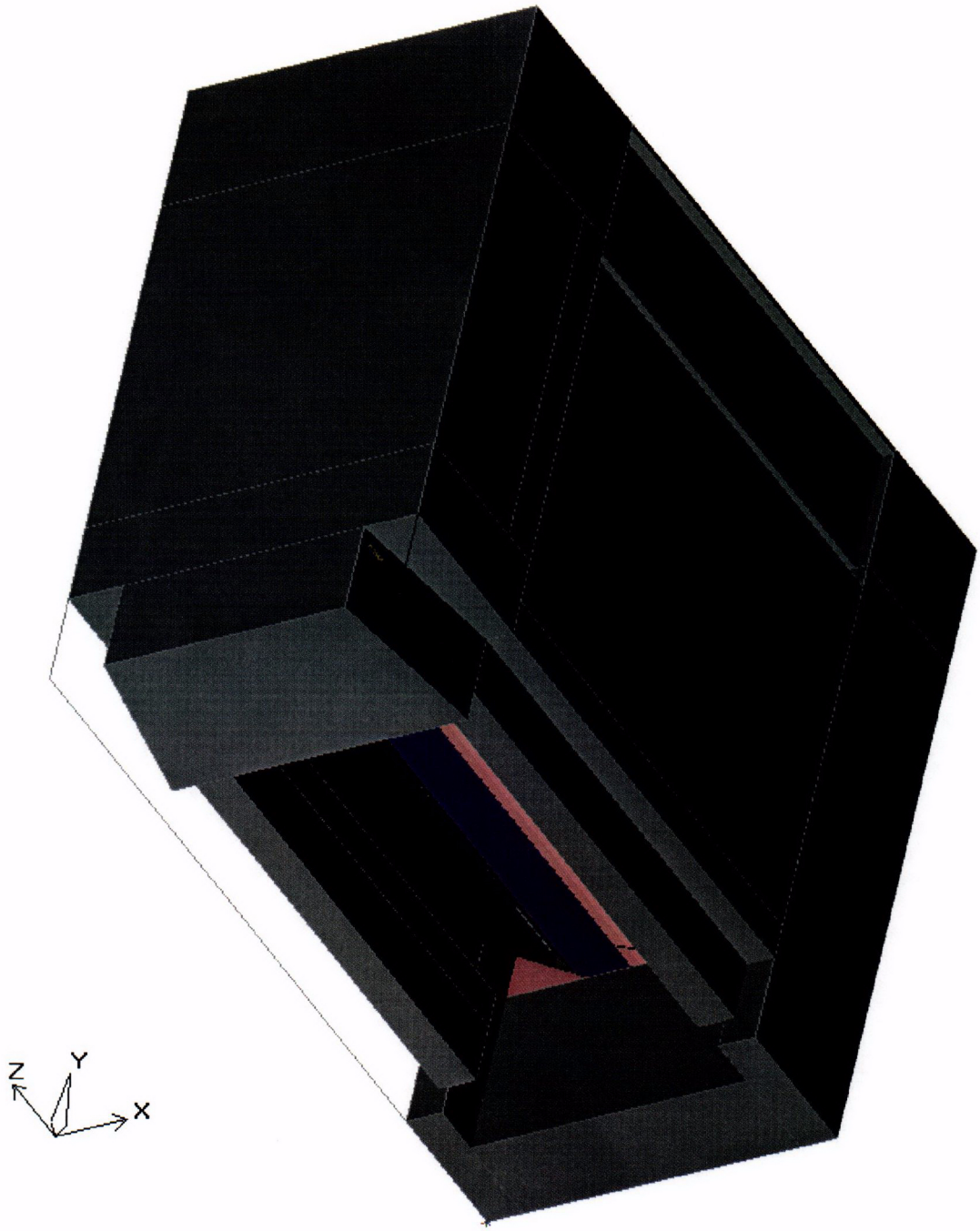

Figure P.4-53 Model View From Underside Of HSM-H

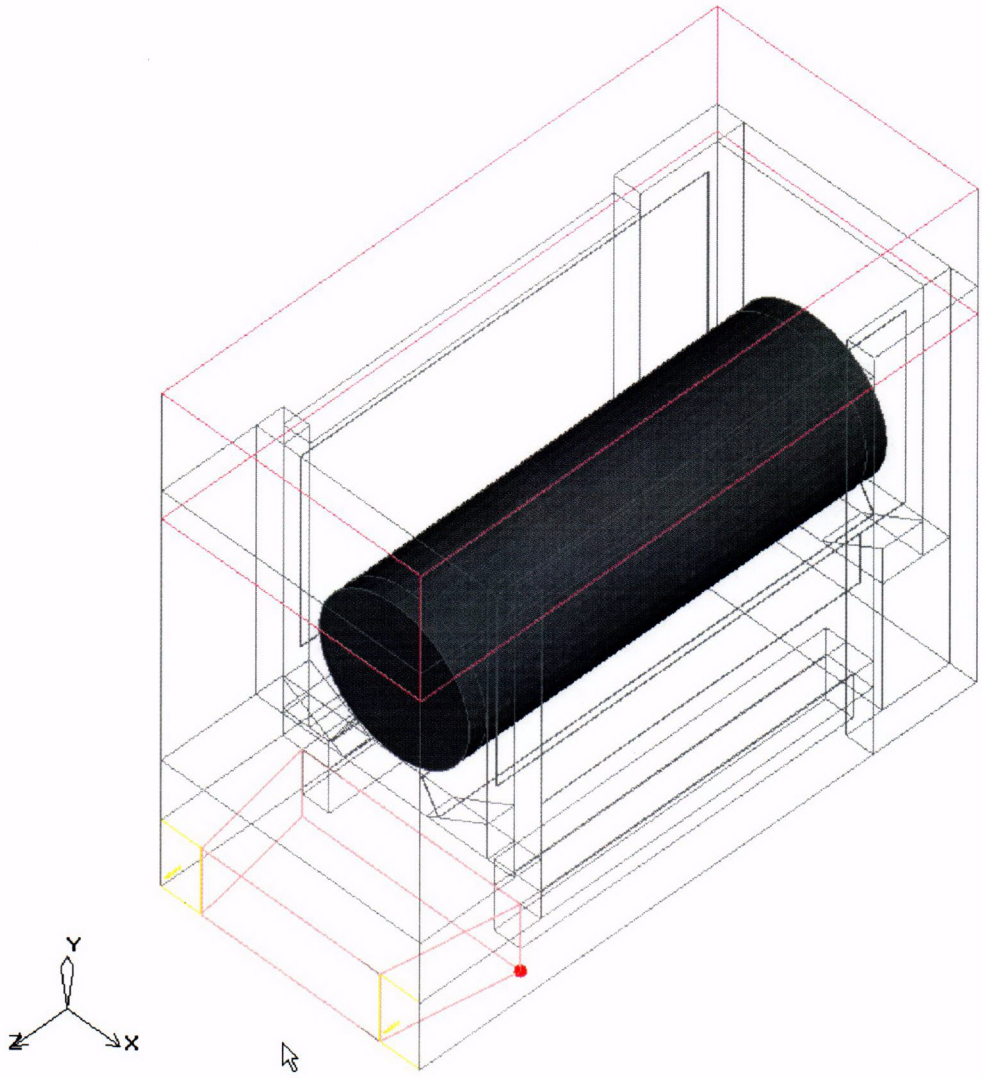

Figure P.4-54 DSC Within HSM-H

C20

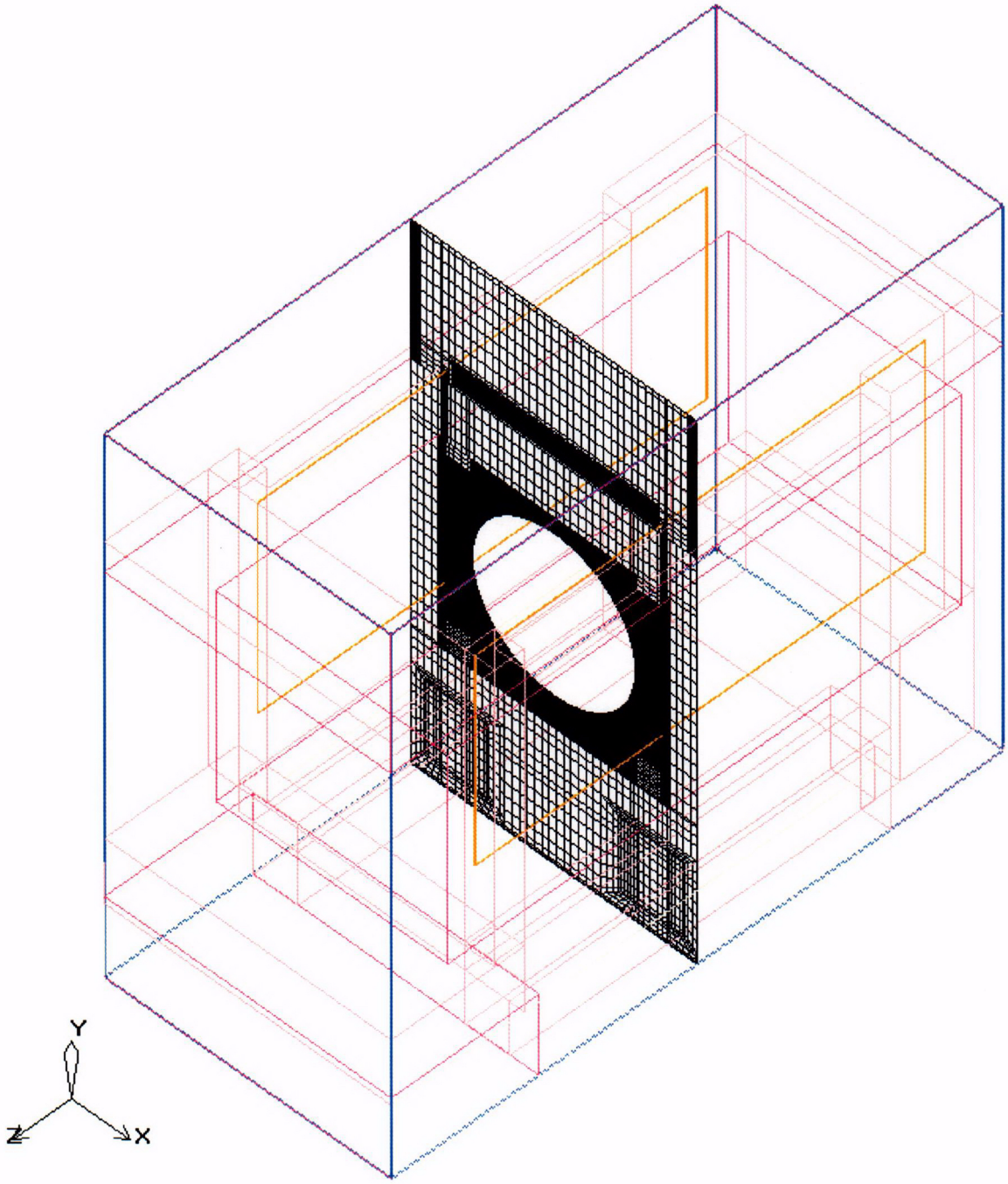

Figure P.4-55 Perspective View Of Meshing At X-Y Plane Of HSM-H

C21